PARAMETRIC STUDY OF WATER-GAS SHIFT REACTION OVER Pt-BASED CATALYSTS

by

Özgür Yaşar Çağlar

B.S., Chemical Engineering, Boğaziçi University, 2013

Submitted to the Institute for Graduate Studies in
Science and Engineering in partial fulfillment of
the requirements for the degree of
Master of Science

Graduate Program in Chemical Engineering

Boğaziçi University

2015

PARAMETRIC STUDY OF WATER-GAS SHIFT REACTION OVER Pt-BASED CATALYSTS

APPROVED BY:

Assoc. Prof. Ahmet Kerim Avcı (Thesis Supervisor)	…….....
Assoc. Prof. Hasan Bedir	…….....
Prof. Ramazan Yıldırım	…….....

DATE OF APPROVAL: 03.08.2015

To my family

ACKNOWLEDGEMENTS

First of all, I would like to express my gratitude to my supervisor Assoc. Prof. Ahmet Kerim Avcı, whose encouragement and guidance enlightened my way during my MS thesis. I am grateful to have the opportunity to work with him and my thesis would not be possible without his dedication.

I would like to thank my thesis committee members, Prof. Ramazan Yıldırım and Assoc. Prof. Hasan Bedir for devoting their valuable time to read and comment on my thesis.

I also want to thank Bilgi Dedeoğlu, Murat Düzgünoğlu, Melike Gürbüz, Başak Ünen and Yakup Bal for their everlasting help. Thanks to Erkan Karabekmez and Bilge Gedik Uluocak for their help in XRD and SEM&EDX analyses conducted at boğaziçi University Research and Development Center.

I would like to thank my friends Serhat Erşahin, Mustafa Türkekul, Melis Yıldırım, Onur Önel, Dilruba İnam and Gülce Güldür for their friendship and endless support. My special thanks to Can Ekici for phenomenal past two years, as roommates, what we shared and tasted were on another level that can not be exceeded.

I would like to present my sincere gratitudes to Elif Erdinç and Coşar Doğa Demirhan for not only their endless support on my thesis but also being an amusing company on this journey. The memories of JLB will be a part of me forever. And yes, it was having like a bunch of super friends.

I would like to thank all Whiskey Night members, Barış Burnak, Coşar Doğa Demirhan, Can Kazan and Fuat Şakirler. In the light of single malts, I hope we will meet at US for a Bourboun Night in Kentucky. Although we are on crossroads now, here's where fun begins.

My special thank goes to Sinan Koç for his guidance during my thesis work. His aids on my study can not be underestimated. I would like to thank Begüm Alaybeyoğlu and Zeynep Erge Akbaş for good memories during lunches.

I would also like to thank Emre Demirel, Elif Can, Elif Gençtürk and Manouchehr Nadjafi and other members of yemekhane group members. The sound of your handclapping will always tingle in my ears.

I would like to thank Melek Selcen Başar, Aysun İpek Paksoy, Aybüke Leba for good moments we shared in KB 403. I would also like to thank Tolga Yardımcı, Utku Deniz, Serdar Özsezen, Ali Uzun, Merve Eropak, Pelinsu Bulutoğlu and Amin Delparish.

I thank to those whom contributed to my existance, I wish I would have thousands of pages to feature them individually. *In a sentimental mood*, I guess I am. Let's cut the chase and finish with one of my favourites, *it is too bad she won't live, but then again who does?*

I devote this thesis to my family whom everlasting support make my work solid. Without their unconditional love and encouragement, it would be impossible for me to complete this challenge.

Financial support for this work is provided by TÜBİTAK through project 113M229.

ABSTRACT

PARAMETRIC STUDY OF WATER-GAS SHIFT REACTION OVER Pt-BASED CATALYSTS

In this study, parametric investigation of low temperature water-gas shift reaction over Pt-based catalysts is carried out. Effects of reaction temperature, feed composition, catalyst particle size and reactor geometry on CO conversion are examined. The catalysts, 1.5 wt% Pt-5 wt% CeO_2/Al_2O_3 and 1 wt% Pt/MIL-53(Al), are prepared by the incipient-to-wetness method using deionized water as solvent. It is observed that CO conversion increases with temperature significantly, whereas it varies slightly with the feed composition. Highest CO conversion of 84 % is obtained at 325 °C and at feed composition including the highest CO_2 content. CO conversions obtained over Pt/MIL-53(Al) remained less than 5 % due to the change in the crystal structure of MIL-53(Al) after impregnation of Pt. XRD analyses reveal that storage conditions of MIL-53(Al) is important to prevent degeneracy in crystal structure and incipient-to-wetness method for catalyst preparation is not suitable for MIL-53(Al). It is found that CO conversion increases from 1 % to 4 % by decreasing the reactor diameter from 10 mm to 2 mm. A similar effect is noted by decreasing particle size of the $Pt/CeO_2/Al_2O_3$ catalyst from $3.02x10^{-1}$ mm to $3x10^{-3}$ mm which increased CO conversion from 1 % to 12 %. These findings indicate that running WGS in a microchannel reactor configuration involving reactor diameters in the sub-millimeter range can improve CO conversion. This hypothesis is also tested in the context of studies in which the reaction is carried out in microchannel reactor configurations involving washcoated and packed forms of the $Pt/CeO_2/Al_2O_3$ catalysts. However, no net findings are obtained due to problems in coating of the catalyst and by-passing of the reactive mixture.

ÖZET

SU-GAZI GEÇİŞ REAKSİYONUNUN Pt-TEMELLİ KATALİZÖRLER ÜZERİNDE PARAMETRİK OLARAK İNCELENMESİ

Bu çalışmada düşük sıcaklık su-gazı geçiş reaksiyonun Pt içeren katalizörler üzerindeki parametrik incelemesi gerçekleştirilmiştir. Reaksiyon sıcaklığının, besleme kompozisyonun, katalizör tanecik boyutunun ve reaktör geometrisinin CO dönüşümü üzerindeki etkileri incelenmiştir. Katalizörler, 1.5 wt% Pt-5 wt% CeO_2/Al_2O_3 and 1 wt% Pt/MIL-53(Al), ardışık emdirme yöntemi ile deiyonize su kullanılarak hazırlanmıştır. CO dönüşümünün sıcaklıkla belirgin bir şekilde arttığı gözlemlenirken, besleme kompozisyonuna göre az miktarda değişim gösterdiği tespit edilmiştir. En yüksek CO dönüşümü olan % 84, 325 °C sıcaklıkta ve CO_2 miktarının besleme akımındaki en yüksek kompozisyonda olduğu şartlarda elde edilmiştir. Pt/MIL-53(Al) için elde edilen CO dönüşümleri, Pt atomlarının emdirilmesinin ardından MIL-53(Al)'nin kristal yapısındaki değişimden ötürü % 5'in altında kalmıştır. XRD analizleri MIL-53(Al)'nin saklama koşullarının kristal yapısındaki değişimi önlemek için önemli olduğunu ve ardışık emdirme yönteminin MIL-53(Al) için uygun bir katalizör hazırlama yöntemi olmadığını ortaya çıkartmıştır. Reaktör çapı 10 mm'den 2 mm'ye azalırken, CO dönüşümünün % 1'den % 4'e arttığı tespit edilmiştir. Benzer bir etki $Pt/CeO_2/Al_2O_3$ tanecik çapının $3.02x10^{-1}$ mm'den $3x10^{-3}$ mm'ye azaltılmasıyla gözlemlenmiş, bu değişiklik ile CO dönüşümü % 1'den % 12'ye artmıştır. Bu bulgular WGS reaksiyonun milimetre altı aralıkta reaktör çapları içeren bir mikrokanal reaktör düzeninde CO dönüşümünün iyileştirilebileceğine belirtmektedir. Bu hipotez $Pt/CeO_2/Al_2O_3$ katalizörünün tanecik formunda ve kaplı bir tabaka halinde bulunduğu değişik mikrokanal reaktör düzenlerinde denenmiştir. Ancak, katalizör tabakasının yeterince kuvvetli şekilde tutunamaması ve reaksiyon karışımının tanecik formundaki katalizör yatağını atlaması gibi problemlerden ötürü net bir bulgu elde edilememiştir.

TABLE OF CONTENTS

ACKNOWLEDGEMENTS iv
ABSTRACT vi
ÖZET vii
LIST OF FIGURES x
LIST OF TABLES xiii
LIST OF SYMBOLS xv
LIST OF ACRONYMS/ABBREVIATIONS xvi
1. INTRODUCTION 1
2. LITERATURE SURVEY 3
2.1. Hydrogen Technology 3
2.2. Water Gas Shift Reaction 5
2.3. Water Gas Shift Catalyst 7
2.4. Metal-Organic Frameworks 12
2.5. Microchannel Reactors 15
3. EXPERIMENTAL WORK 17
3.1. Materials 17
3.1.1. Chemicals 17
3.1.2. Gases and Liquids 17
3.2. Experimental Systems 18
3.2.1. Catalyst Preparation Systems 19
3.2.2. Catalyst Characterization System 19
3.2.3. Catalytic Reaction System 20
3.2.4. Product Analysis System 21
3.3. Catalyst Preparation and Pretreatment 23
3.3.1. Catalyst Preparation 23
3.3.2. Catalyst Coating on Microchannel Plates 24
3.4. Reaction Tests 25
3.4.1. Blank Tests 25
3.4.2. WGS in Packed Bed Reactor 25

3.4.3. WGS in Microchannel Reactor 27
3.4.4. WGS in 2 mm ID Quartz Reactor 30
4. RESULTS AND DISCUSSIONS 33
4.1. WGS Reaction over Pt/CeO_2/Al_2O_3 for Packed Configuration 33
4.2. WGS Reaction over Pt/MIL-53(Al) for Packed Configuration 36
4.3. WGS Reaction over Pt/CeO_2/Al_2O_3 for Microchannel Configurations 39
4.4. Investigation of Reactor and Catalyst Configuration on WGS Reaction over Pt/CeO_2/Al_2O_3 43
4.5. Catalyst Characterization 45
4.5.1. XRD Results 45
4.5.1. 1. MIL-53(Al) 45
4.5.1. 2. 1.5 wt% Pt/MIL-53(Al) 47
4.5.2. SEM/EDX Results 48
5. CONCLUSIONS AND RECOMMENDATIONS 53
5.1. Conclusions 53
5.2. Recommendations 54
APPENDIX A: MFC CALIBRATION CURVES 56
APPENDIX A: GC CALIBRATION CURVES 59
REFERENCES 62

LIST OF FIGURES

Figure 3.1. Impregnation system. 19

Figure 3.2. Schematic representation of the reaction system. 21

Figure 3.3. Schematic Diagram of the Packed Bed Reactor and Furnace System. 25

Figure 3.4. Coated Microchannel Reactor Configuration. 28

Figure 3.5. Packed Microchannel Reactor. 28

Figure 3.6. Schematic Diagram of the 2 mm ID Packed Bed Reactor and Furnace System. 30

Figure 4.1. Results for Effect of Temperature on CO Conversion for All Cases over 1.5 wt % Pt –5 wt% CeO_2 / Al_2O_3. 34

Figure 4.2. Results for Effect of Feed Composition on CO Conversion for All Temperatures over 1.5 wt % Pt –5 wt% CeO_2 / Al_2O_3. 35

Figure 4.3. Results for Effect of Temperature on CO Conversion for All Cases over 1 wt.% Pt/MIL-53(Al). 37

Figure 4.4. Results for Effect of Feed Composition on CO Conversion for All Temperatures over 1 wt.% Pt/MIL-53(Al). 38

Figure 4.5. FeCrAlY plates. 40

Figure 4.6. Results for Effect of Feed Composition on CO Conversion at 300 °C for 3-micron Pt/CeO_2/Al_2O_3 Packed Reactor Configuration. 41

Figure 4.7. Results for Effect of Reactor Diameter and Catalyst Particle Size on CO Conversion over WGS Reaction. 43

Figure 4.8. XRD Result for Fresh Untreated MIL-53(Al). 46

Figure 4.9. XRD Results for Old Untreated MIL-53(Al) and Fresh Untreated MIL-53(Al). 46

Figure 4.10. XRD Result for Unused1.5 wt% Pt/MIL-53(Al) Catalyst. 47

Figure 4.11. XRD Results for Untreated MIL-53(Al) and Unused1.5 wt% Pt/MIL-53(Al) Catalyst. 48

Figure 4.12. SEM image for freshly reduced 3-micron sized 1.5 wt % Pt–5 wt% CeO_2/Al_2O_3 catalyst (500x). 49

Figure 4.13. SEM image for freshly reduced 3-micron sized 1.5 wt % Pt–5 wt% CeO_2/Al_2O_3 catalyst (10000x). 49

Figure 4.14. Mapping of freshly reduced 3-micron sized 1.5 wt % Pt–5 wt% CeO_2/Al_2O_3 catalyst. 50

Figure 4.15. SEM image for freshly reduced 0.3 mm particle sized 1.5 wt % Pt–5 wt% CeO_2/Al_2O_3 catalyst (50x). 51

Figure 4.16. SEM image for freshly reduced 0.3 mm particle sized 1.5 wt % Pt–5 wt% CeO_2/Al_2O_3 catalyst a. Magnified 5000x b. Magnified 2000x. 51

Figure 4.17. SEM image for spent 0.3 mm particle sized 1.5 wt % Pt–5 wt% CeO_2/Al_2O_3 catalyst (50x). 52

Figure 4.18. SEM image for spent 0.3 mm particle sized 1.5 wt % Pt–5 wt% CeO_2/Al_2O_3 catalyst a. Magnified 2000x b. Magnified 10000x. 52

Figure A.1. MFC Calibration Curve of H_2. 57

Figure A.2. MFC Calibration Curve of CO. 58

Figure A.3. MFC Calibration Curve of CO_2. 58

Figure A.4. MFC Calibration Curve of N_2. 59

Figure B.1. GC Calibration Curve for H_2. 60

Figure B.2. GC Calibration Curve for CO. 61

Figure B.3. GC Calibration Curve for CO_2. 61

Figure B.4. GC Calibration Curve for N_2. 62

LIST OF TABLES

Table 3.1. Chemicals used for catalyst preparation. 17

Table 3.2. Specifications and applications of the liquids used. 18

Table 3.3. Specifications and applications of the gases used. 18

Table 3.4. Gas analysis conditions for product gas stream. 22

Table 3.5. Operating conditions for WGS reaction in the study for packed configuration. 26

Table 3.6. Feed conditions for WGS reaction in the study. 26

Table 3.7. Experimental road map for WGS reaction in the study for packed configuration. 27

Table 3.8. Operating conditions for WGS reaction in the study for micro packed configurations. 29

Table 3.9. Experimental road map for WGS reaction in the study for micro packed configuration. 29

Table 3.10. Operating conditions for WGS reaction in the study for 2 mm ID Quartz Reactor. 31

Table 3.11. Experimental road map for WGS reaction in the study for 2 mm ID Quartz Reactor. 31

Table 4.1. Conversions for Packed Configuration over $Pt/CeO_2/Al_2O_3$. 36

Table 4.2. Conversions for Packed Configuration over Pt/MIL-53(Al). 39

Table 4.3. Conversions for Packed Reactor Configuration over 3-micron $Pt/CeO_2/Al_2O_3$ at 300 °C. 42

Table 4.4. Conversions for Different Packed Reactor Configurations over $Pt/CeO_2/Al_2O_3$ catalyst. 43

LIST OF SYMBOLS

C_{CO}^{in}	CO concentration in feed
C_{CO}^{out}	CO concentration in outlet
ΔG^0	Gibbs free energy of reaction (kj/mol)
H	Height of the microchannel (mm)
K_{eq}	Equilibrium constant
L	Length of the microchannel (mm)
T	Temperature (°C)
W	Width of the microchannel (mm)
ΔH^0	Standart enthalpy of reaction (kj/mol)

LIST OF ACRONYMS/ABBREVIATIONS

AFC	Alkaline Fuel Cell
ATR	Auto-Thermal Reforming
DI	Deionized
DMFC	Direct Methanol Fuel Cells
GC	Gas Chromatograph
HKUST	Hong Kong University of Science And Technology
HPLC	High Performance Liquid Chromatography
ID	Inner Diameter
HTS	High Temperature Shift
LTS	Low Temperature Shift
MCFC	Molten Carbonate Fuel Cell
MFC	Mass Flow Controller
MIL	Material Institute Of Lavoisier
MOF	Metal-Organic Framework
MTS	Medium Temperature Shift
NCCs	Nitrogen-Containing Compounds
PAFC	Phosphoric Acid Fuel Cell
PEMFC	Proton Exchange Membrane Fuel Cell
POX	Partial Oxidation
S/C	Steam-to-Carbon Ratio
SCCs	Sulfur-Containing Compounds
SEM	Scanning Electron Microscopy
SMR	Steam Methane Reforming
SOFC	Solid Oxide Fuel Cell
TCD	Thermal Conductivity Detectors
W/F	Catalyst Weight to Feed Flow Rate
WGS	Water Gas Shift
XRD	X-Ray Diffraction

1. INTRODUCTION

Fossil fuels, especially crude oil, are the main and widely most used energy source in worldwide. Due to industrial growth and increasing trend of population, the demand of energy increases drastically. Importance of renewable energy sources, which is the biggest alternative of crude oil, become vital due to the decrease in crude oil wells and increased cost of bringing crude oil to the surface. Renewable energy sources address the main drawback of the crude oil usage, emission of carbon dioxide. There are several alternative energy sources like wind, hydro and solar energy. However, their applications do not eliminate the dependency of crude oil in their current technology level. Another promising clean technology is using hydrogen to generate energy in fuel cells. It is expected that hydrogen utilized fuel cells can eliminate the fossil fuel dependency.

The proton exchange membrane fuel cells (PEMFC) can be used in transportation, and in primary power generation in future. It is expected that PEMFC will eliminate crude oil dependency consequently (Chen *et al.*, 2008.). The main energy source of PEMFC is hydrogen, which is mostly obtained via catalytic partial oxidation or steam reforming of hydrocarbons. However, the most critical issue in PEMFC is the poisoning of fuel cell catalyst by impurities such as CO. Anode of the PEMFCs cann be deactivated irreversibly at CO level of higher than 10 ppm (Zalc *et al.*, 2002.). In order to address this problem, water-gas shift (WGS) reaction is utilized for reducing the CO level below 10 ppm. WGS reaction, given in Equaiton 1.1, is the most promising method to decrease the CO level:

$$CO + H_2O = CO_2 + H_2, \qquad \Delta H^o = -41.2 \text{ kJ/mol}, \quad \Delta G^o = -28.6 \text{ kJ/mol} \qquad (1.1)$$

The reaction defined in two separated names as low temperature water gas shift (LT-WGS) reaction (190-250 °C) and high temperature water gas shift (HT-WGS) reaction (350-450 °C). Due to the exothermic behavior of the reaction, formation of H_2, the valuable product, is thermodynamically favored at low temperatures. On the other hand, the reaction is kinetically favored at high temperatures. In order to obtain the both high activity and H_2 production, different catalysts are explored. There are four general types of WGS catalysts, however, precious metal-based catalysts, mainly platinum and gold have

been investigated for fuel cell applications. It is observed that the precious metal-based catalysts (mainly Pt, Rh, Ru, Au, and Pd are deposited on partially reducible oxides such as ceria, zirconia, titania, iron oxides, and mixed oxides of ceria, like ceria- zirconia) are quite active in 250-400 °C range (Ratnasamy and Wagner, 2009).

Metal-organic frameworks (MOFs) are referred as several names such as porous coordination polymers (PCPs), and porous coordination networks (PCNs) etc.. The studies on MOFs are incrementing over the past decade. Their applications on gas storage (H_2, CH_4 etc.), gas/vapor separation, heterogeneous catalysts, luminescent and fluorescent materials are promising due to their high surface area, which is up to 5900 m^2 g^{-1} (Kuppler *et al.*, 2009; Czaja *et al.*, 2009). MOFs provide both stable and ordered structure in high surface areas because they possess both organic and inorganic structures.

The most important issue to be solved for fuel cells is the requirement of small size reactor. Microchannel reactors can address the mobile application problems of fuel cells. High surface area to volume ratios of microchannel reactors makes this reactor type attractive for fuel cell application. The ratio is up to 50000 m^2/m^3, which is only 1000 m^2/m^3 in conventional reactors. Moreover, microchannel reactors provide fast and uniform heat transfer rates, which are significant for WGS reaction (Ehrfeld *et al.*, 2001).

The aim of the present study is to carry out a parametric investigation of LT-WGS over Pt-based catalysts. In addition to the effect of parameters such as reaction temperature, feed conditions and catalyst particle size, the impact of various catalysts ($Pt/CeO_2/Al_2O_3$ and Pt/MOF) and reactor geometry on CO conversion are investigated for exploring the possible effects of reactor structuring and of using MIL-53(Al), a MOF structure. The study contains five chapters. Chapter 2 includes literature survey on hydrogen technology, WGS reaction, WGS catalysts, MOF materials and microchannel reactors. Chapter 3 consists the catalyst preparation techniques, experimental system introduction and reaction tests. In Chapter 4, results and discussion are presented. The major conclusions and recommendations for future works are given in Chapter 5.

2. LITERATURE SURVEY

2.1. Hydrogen Technology

Today's energy and transport system, which is based mainly on fossil energy carriers, can in no way be evaluated as sustainable. Oil and gas still make the world work; fossil fuels still account for about 80% of today's global primary energy supply. The increasing global demand for fuel is one of the main reasons for the rise in greenhouse gas emissions. Emissions of CO_2, the main greenhouse gas from human activities, are the subject of a worldwide debate about energy sustainability and the stability of the global climate. Evidences that human activities are causing the planet to warm up are now unequivocal according to the Intergovernmental Panel on Climate Change (IPCC) (Ball and Wietchelb, 2009). Drawbacks of fossil energy usage can be addressed by using hydrogen as an energy source. Hydrogen is a promising energy source for a sustainable future due to its air pollution and greenhouse gas emmission free properties. Moreover, unlike wind or solar energy hydrogen can be stored and transported. Hence, it is considered as a viable energy carrier in the future. In particular, recently there is a progressive development in fuel cells, which can be used for transportation, primary power generation and distributed generation and it is known that hydrogen is a vital fuel in the fuel cells (Chen *et al.*, 2008).

Over the years, there has been a significant progress in the development of fuel cells. A number of fuel cells, such as the proton exchange membrane fuel cell (PEMFC), the alkaline fuel cell (AFC), the direct methanol fuel cells (DMFC), the phosphoric acid fuel cell (PAFC), the molten carbonate fuel cell (MCFC) and the solid oxide fuel cell (SOFC), are likely to be commercialized and applied in industries in the near future. In these fuel cells, a variety of feed stocks such as methanol, ethanol, natural gas, syngas or hydrogen can be used. PEMFCs are considered as the most suitable for energy production, where the raw material is hydrogen. It is expected that PEMFC will eliminate crude oil dependency consequently (Chen *et al*., 2008).

Hydrogen is also a crucial raw material in industry, mainly is used for ammonia synthesis, the breaking down of heavier crude oils and the removal of sulfur. Hydrogen is mainly genereted from water, biomass, natural gas and coal (Turner, 2004). Nowadays, the H_2 production is dominated by steam reforming of natural gas, which is mainly comprised of methane. (Trimm, 2005) Steam reforming of methane (SMR) is given in Equation 2.1. Besides the steam reforming, partial oxidation (POX) and auto-thermal reforming (ATR) of methane are another conventional ways to produce hydrogen, which are given in Equation 2.2 and 2.3:

SR: $$CH_4 + H_2O \leftrightarrow CO + 3H_2 \qquad \Delta H > 0 \qquad (2.1)$$

POX: $$CH_4 + \frac{1}{2}O_2 \leftrightarrow CO + 2H_2 \qquad \Delta H < 0 \qquad (2.2)$$

ATR: $$CH_4 + \frac{1}{2}H_2O + \frac{1}{4}O_2 \leftrightarrow CO + \frac{5}{2}H_2 \qquad \Delta H < 0 \qquad (2.3)$$

Product streams of aforementioned reactions are called syngas, which is comprised of CO and H_2. The product streams of reforming reactions contain high CO levels, particularly product stream contains 1-10% of CO for SMR. (Dae-Woon *et al.*, 2014) In order to utilize H_2 from SMR for fuel cell applications, CO levels should be decreased because CO level higher than 10 ppm has a poisoning effect on fuel cell catalyst, which could be deactivated irreversibly at high level of CO. (Zalc *et al.*, 2002).

There are several methods to reduce the CO levels of syngas for fuel cell applications, namely membrane separation process, pressure swing adsorption process and water gas shift reaction. Former two methods have high limitations for cost and control of the process, whereas the water gas shift (WGS) reaction provides an ideal solution decreasing CO levels to 0.5-1 % for product stream of SMR reaction. After the WGS reaction, the desired level of CO could be achieved by POX of methane or selective methanation of CO. (Lenite *et al.*, 2011)

2.2. Water Gas Shift Reaction

The first report of the WGS reaction (Equation 1.1) was published in 1888 and described how the mixture of carbon monoxide and water vapor is converted to carbon dioxide and hydrogen (Rhodes *et al.*, 1995). The demand of WGSR is raised from increase in demand of hydrogen for industrial use such as Haber-Bosch ammonia synthesis. The demand of hydrogen for Haber process was obtained by coal or coke gasification, however, during the reaction side product CO had to be removed by liquefaction or copper liquor scrubbing. Since these operations were not efficient or cheap, a catalytic process was needed to remove the CO from the mixture. This is where WGSR stepped in. It was discovered that the oxides of iron and chromium could convert the CO in the mixture from Haber process to CO_2 and H_2 in presence of steam according to Equation 1.1. As a result, additional hydrogen was generated as the undesired CO is removed simultaneously. The iron oxide and chromium oxide type catalysts still form the basis for today's high temperature catalyst (Rhodes *et al.*, 1995; Ratnasamy and Wagner, 2009).

The WGSR is also used in methanol synthesis and in Fischer-Tropsch process, where it is used to attain the desired levels of H_2/CO ratio. Another common usage is to eliminate the large amounts of CO coming from SMR, which is primary method to produce H_2 for fuel cells. However, the product from SMR contains 1-10% of CO, which is harmful to fuel cell because above 10 ppm of CO, it deactivates (Jeong *et al.*, 2014). Therefore, reformed gas must be removed from large CO for fuel cell operations. Furthermore, the estimations show that about 10% of worldwide yearly energy consumption will be obtained from WGS reaction by the year 2030 (Noor *et al.*, 2014).

The reaction is not affected by pressure since there is no change in volume from reactants to products. It is also a moderately exothermic reversible reaction and conversion is equilibrium controlled. The equilibrium constant is given in Equation 2.4 and it decreases with increasing temperature. Consequently, high conversions are favored at low temperatures. However, at high temperatures, the reaction is kinetically favorable. In order to achieve high conversions, both kinetically and thermodynamically favorable region of the reaction should be taken into consideration. As a solution, utilization of two WGS reactor in series is developed, where the reaction is occurred both high and low

temperatures. In the first part, the operating temperature is between 350-450 °C, therefore, called high temperature shift (HTS), whereas in second part the reaction is taken place as low temperatures in range of 190 to 250 °C and called low temperature shift (LTS) (Smith *et al.*, 2010).

$$K_{eq} = exp\left(\frac{4577.8}{T(K)} - 4.33\right) \tag{2.4}$$

In conventional usage, high amounts of CO from reformed gas are reduced to concentrations to around 2-5% with HTS for fuel cell applications. Following a LTS, the CO concentration of 0.5 to 1 % could be achievable with WGS reaction. In order to reach the desired levels of CO for fuel cell applications, a POX reactor is added conventionally to the end of WGS reactors (Luengnaruemitchai *et al.*, 2003).

The effects of steam-to-carbon (S/C) and amount of H_2 in reformate on equilibrium CO concentration as a function of temperature are well investigated in the literature. A higher S/C ratio results lower CO equilibrium concentrations at a given temperature. Moreover, a higher S/C ratio provides same CO equilibrium concentration at a higher temperature with respect to a lower S/C ratio, which results reduction of reactor size due to the more favorable kinetics at high temperature. The presence of H_2, on the other hand, favors the backward reaction and results in higher CO equilibrium concentrations. In order to achieve the desired levels of CO concentration at equilibrium concentrations, lower temperatures or higher S/C ratios can be utilized (Shekhawat *et al.*, 2011; Ratnasamy and Wagner, 2009).

In parallel to WGS reaction, so called methanation reaction, Equation 2.5, can take place:

Methanation: $CO + 3H_2 = CH_4 + H_2O \qquad \Delta H^{\circ}_{298} = -206.2\ \mathrm{kJ/mol}$ (2.5)

Methanation is an undesired reaction during WGS because the hydrogen is consumed. Consequently, overall production of hydrogen decreases as the methanation

occurs. The catalysts investigated for WGS reaction are introduced in the following section.

2.3. Water Gas Shift Catalysis

The WGS catalysts can be investigated under two main groups as HTS and LTS catalysts. However, there are some other WGS catalyst types, namely ones that employ cobalt and molybdenum sulfides as the active ingredients, ones called as medium temperature shift (MTS) catalyst that operate at temperatures between those of HTS and LTS catalysts, and lastly, precious metal-based catalysts, mainly platinum and gold, all of which are studied for their possible use in fuel cell applications (Ratnasamy and Wagner, 2009).

The HTS catalysts are the oldest catalysts used in the WGS reaction. The iron-chromium (Fe/Cr) oxide was first patented as a WGS catalyst by Bosh and Wild in 1914. Although nearly a century has passed, Fe/Cr is still utilized as a primary catalyst for HTS because of its reasonable activity and durability in most applications (Lee *et al.*, 2013). The pre-activated catalyst is generally composed of 87–95% Fe_2O_3 (ferric oxide, mineral name: hematite), 5–10% Cr_2O_3 (chromium (III) oxide) and miscellaneous other components, such as CuO, Co_2O_3 and/or MgO. The addition of low percentages of chromium to the iron helps the catalyst to stabilize and to extent its life by decreasing sintering. At high temperatures, sintering or aggregation of particles cause a decrease in surface area and overall catalyst activity. Moreover, the other components like Cu are added to increase the activity of Fe/Cr catalyst by decreasing the activation energy and increasing the selectivity of the catalyst (Lee *et al.*, 2013). The promotion of Fe/Cr catalysts can be done by varying the amounts of Cu, Pb, Ba, Ag or Hg. All result in increase in the activity with the order of Hg>Ag~Ba>Cu>Pb (LeValley *et al.*, 2014).

The CO concentration leaving a conventional Fe/Cr WGS reactor can be as low as 3% by volume CO, where the inlet concentration of CO to the reactor is 10-15%. The concentration of hydrogen fed to this catalytic system must be minimized due to the extremely exothermic nature of the reduction reaction which can cause temperature spiking and subsequent sintering (Rhodes *et al.*, 1995; Keiski and Salmi, 1992). The Fe/Cr catalyst

is used in a process for an average of 3–5 years without exchanging with fresh catalyst (Lee *et al.*, 2013). HTS catalysts have the advantages of low cost and long life, and reasonable resistant to Sulphur. However, they are not active below 350 °C and they have to pre-treated before usage after exposure to air due pyrophoric nature. In addition, they require reduction and stabilization by surface oxidation (Trimm, 2005; Callaghan, 2006).

The usage of LTS catalysts originates to 1960s. The development of highly efficient sulfur removal technologies in ammonia synthesis allowed the usage of sulfur-sensitive Cu-ZnO catalysts at sufficiently low temperatures for WGS reaction, which results in achieving equilibrium CO concentration below 0.3 % at the exit of the LTS reactors. The early usage of Cu in WGS reaction confronted with easy sintering, but, it is overcomed by using various stabilizers, like SiO_2, Cr_2O_3. However, the introduction of Cu-ZnO catalyst and later Cu-ZnO-Cr_2O_3 and Cu-ZnO-Al_2O_3 catalyst enabled the production of catalysts with high and stable copper surface areas, which result in usage of this catalyst in hydrogen production operations (Ratnasamy and Wagner, 2009).

The typical composition of a commercial Cu-ZnO-Al_2O_3 catalyst is 33% CuO, 34% ZnO and 33% Al_2O_3. The advantages of the low temperature catalyst are its selectivity and fewer side reactions occurring at higher operating pressures. The normal life time of the low temperature catalyst is 2 – 3 years (Rase, 1977). LTS catalysts are unstable above 300 °C, and they are pyrophoric if exposed to air. Moreover, they are highly sensitive to the Sulphur. Therefore, the drawbacks of copper based catalyst have been overcomed by use of precious metal based catalyst (Trimm, 2005).

For compact fuel cell applications, it is suggested that use of noble metals as catalysts can help to cope with the disadvantages of the existing commercial WGS catalysts. Many catalyst configurations are investigated and the most studied ones are precious metals, such as Pt, Ru, Rh, Au and Pd, deposited on partially reducible oxides such as ceria, zirconia, titania, iron oxides and mixed oxides of ceria, like ceria- zirconia.

One of the precious metals used for WGS catalyst is gold. Although gold based catalysts are regarded as poorly active catalysts, when it is deposited in the form of nano-particles on metal oxides, it provides high catalytic activity. Gold is considered as a good

candidate for abatement of CO for WGS reaction due to high activity and relatively low cost with respect to other precious metals like Pt or Rh (Lenite *et al.*, 2011). The main drawbacks of Au are the particles should be well-dispersed over the support material in order to obtain activity (Castano *et al.*, 2014).

Ceria or cerium oxide has been investigated extensively and the results show that it is a promising promoter and support for WGS reaction catalyst. Ceria-based catalyst should involve small diameter particles with high surface area to deliver high activity (Fu *et al.*, 2005). Ceria catalysts provide high oxygen storage capacity, a measure of how much oxygen a support can lend to the reaction. The high oxidation potential of ceria catalysts is also beneficial due to the redox reaction mechanisms involved in WGS reaction (LeValley *et al.*, 2014).

Ceria particle size is another critical aspect that has an important effect on the WGS reaction activity. The size of the ceria particles affects the amount of oxygen storage available to the reaction; however, small ceria particles with large gold particles are capable of achieving high conversion, whereas similar sized ceria particles alone offer almost no conversion. There is a correlation between particle sizes of both the metal and the ceria support, and the activity. Therefore it is crucial to control both the size of the metal and the ceria support in all preparation methods (Fu *et al.*, 2001).

In addition to precious metals, various rare earth metals have been widely studied. Rare earth metals are well known for their catalytic effects, and when added to ceria catalyst, they provide improved thermal stability and increased activity (Wang *et al.*, 2010). Wang et al. (2011) investigated a ceria/zirconium catalyst doped with rare earth metals La, Nd, Pr, Sm, and Y and found that all of the metals increased activity. Moreover, the best selectivity performances have been observed with La, Nd, and Pr. Rare earth metal doping has also been applied to gold/ceria catalyst, where doping with lanthanum and gadolinium have both shown increased activity (Fu *et al.*, 2005).

Aluminum is another common support for WGS catalysts. It is mainly used in LTS with Cu and Zn, and provides high conversions between 200 °C and 240 °C. Au/Al

catalysts have also been previously investigated, but were shown to have poor activity for the WGS reaction. (Lenite *et al.*, 2011)

Nickel aluminum catalysts are traditional catalyst for WGS reaction. The utilization of potassium promoter on these catalysts demonstrated higher selectivity towards CO_2. In addition, potassium impregnated nickel is found to provide more activity and less carbon deposition compared to traditional nickel catalyst. Nickel WGS catalysts often catalyze the methanation reaction which consumes hydrogen and therefore severely decreases total hydrogen production. Promotion of potassium addresses undesired methanation reaction while maintaining the high conversion of CO (Hwang *et al.*, 2011; Kim *et al.*, 2008).

Alumina is used as a stabilizing agent in Au/CeO_2 catalyst. The main role of alumina is that of a textural promoter in stabilizing the Au and ceria crystallites against agglomeration during the WGS reaction and, thereby, maintaining a high catalytic activity in the steady state. The addition of alumina to ceria results in smaller ceria crystallites and, consequently, an increase in the number of oxygen vacancies and oxygen storage capacity of ceria, as estimated from temperature programmed reduction experiments. (Andreeva *et al.*, 2007)

It has been known that platinum group metal provides high activity on WGS reaction; however, their application on commercial approaches is precluded due to their high price. The activity of Pt on WGS has been investigated over different supports, such as CeO_2, TiO_2 and ZrO_2 supports (Azzam *et al.*, 2007) Results show that Pt on TiO_2 provides the highest activity among the others. Carbon formation is observed for Pt over TiO_2 study, which concludes deactivation of the catalyst. It is suggested that the main reason for deactivation is occurred due to sintering of Pt atoms on support. In order to minimize the sintering, Re is added to the Pt/TiO_2 catalyst. The activity is ranked from descending order as $TiO_2 > CeO_2 > ZrO_2$ (Kim *et al.*, 2010). On the other hand, the activity of Au over different supports is another significant issue, which is investigated by separate groups. The results show that the activity with the order of $CeO_2 > TiO_2 > Fe_2O_3 > ZrO_2$ (Kim *et al.*, 2010).

Kalamaras *et al.* (2011) investigated the effect of particle size of Pt metal on WGS reaction. The turn over frequency of WGS was found to change slightly with Pt particle size in range of 1.3 to 8 nm, whereas the specific reaction rate increased with platinum loading and mean particle size of the catalyst.

A study is carried out for comparison of Cu- and Pt-based WGS catalyst. (Kam *et al.*, 2010) The Pt based catalyst showed resistance to chlorine and sulfur poisoning, whereas Cu based catalyst failed. Moreover, the pyrophoric nature of Cu based catalyst was another disadvantage of it, whereas Pt based catalysts showed no pyrophoricity. Last of all, daily start-ups and shut-downs (DSS) operation property of catalysts Cu/ZnO, Pt/CeO_2, Pt/TiO_2 and Pt/ZrO_2 are investigated. Cu/ZnO lost its cativity during the DSS operation. On the other hand, Pt/CeO_2 attained its activity during DSS operation. However, Pt/TiO_2 and Pt/ZrO_2 encountered with sintering, at steady-state operation, consequently, activity loss was obtained.

Boaro *et al.* (2009) have compared Au and Pt on zirconia and ceria-zirconia. Gold showed higher activity at low temperatures compared to platinum. The calcination temperature was another parameter that was studied. In case of Pt a gradual improvement of the performance was observed as the calcination temperature was increased to 823 K, whereas increase in calcination temperature caused a decrease of activity in the case of Au. The possible reason was the sintering of the gold particles that caused increase of size of the molecule. Another significant difference between Au and Pt systems was related to the effect of morphology of support (Boaro *et al.*, 2009). The activity of gold catalysts was almost independent on the surface area of supports whereas the activity of platinum catalysts improves, especially in the range of light-off temperatures, when platinum has been dispersed on oxides with a high surface area.

Wheeler *et al.* (2004) studied the possibility of the WGS reaction using noble metals and metals with ceria in the temperature range of 300 °C to 1000 °C on alumina support. The results show that the activity of the metals in the order of Ni>Ru>Rh>Pt>Pd in absence of ceria. The addition of ceria to the noble metals has led to an increase in the activity of noble metals. The study indicates that the Pt/ceria is the most promising candidate in terms of promotion, stability and lack of methanation activity.

Thinon *et al.* (2008) focused on several precious metals (Pt, Rh, Ru, Au) and Cu over different supports (Al_2O_3, CeO_2, TiO_2, ZrO_2, Fe_2O_3). The highest activity at 300 °C was reported to be on Pt/TiO_2, followed by Pt/CeO_2-Al_2O_3 and Au/CeO_2. Rh and Ru based catalysts showed significant amounts of methane formation. The Au and Cu based catalysts showed promising results for LTS applications due to low activation energy requirement. On the other hand, Pt based catalysts provided high activity at HTS reaction range. Feed of all experiments conducted at typical reformate conditions, and the results indicate that presence of H_2 and CO_2 have negative effects on activity of tested catalysts.

Apart from the noble metals and Au, other transition metals, such as cobalt and nickel have also been investigated as WGS catalysts. They, however, cause methanation, Equation 2.5, of CO to CH4 under typical WGS reaction conditions, especially, below 350 °C (Ratnasamy and Wagner, 2009).

2.4. Metal-Organic Frameworks

The metal-organic framework (MOF) research dates back to 1989 when Hoskins and Robson reported a new class of solid polymeric materials, now known as metal organic framework or coordination polymers, which are crystalline and particulate, and constructed by inorganic metal clusters and multi-dentate organic ligands through coordination connection between them (Hoskins and Robson, 1989). MOFs have received tremendous attention due to their unique structural properties such as high porosity, high surface area per grams of MOF and various tailoring options according to the objective of interest. Their applications are mainly conducted on storage technologies, separation via selective adsorption and catalysts.

MOFs are extensively investigated for hydrogen storage applications. The desired hydrogen storage materials should provide high volumetric and gravimetric storage capacities, fast kinetics, favorable thermodynamics, low desorption temperature, excellent reversibility, long-term cyclic stability and low cost. MOFs can store substantial amounts of hydrogen at cryogenic temperatures. It was reported that NU-100 could store hydrogen up to 99.5 mg g^{-1} (approximately 9 wt. %) hydrogen at 56 bar and 77K (Farha *et al.*, 2010). The adsorption of the hydrogen at cryogenic temperatures, such as 77 K, occurs by

physisorption involving weak van der Waals forces. Considerable research efforts are focused on improving the hydrogen storage characteristics of wide variety of MOFs not only cryogenic temperatures but also at ambient temperature. Generally, very low hydrogen uptakes (< 1 wt. %) have been reported for a wide range of MOFs at room temperature. The reason is that the van der Waals forces which are responsible for physisorption are weak; consequently, the hydrogen storage capacities of adsorbents are low at room temperature. It has been shown from theory that in order to maintain high hydrogen storage capacity at room temperature an isosteric heat of hydrogen adsorption of 15–25 kJ mol^{-1} is required of the material (Langmi *et al.*, 2014).

One of the applications of MOFs is removal of nitrogen-containing compounds (NCCs), sulfur-containing compounds (SCCs), which are widely known contaminants in petroleum refining and in fuels. It is crucial to remove these components before commercial use due to environmental concerns and hazardous effects on catalysts (Khan *et al.*, 2013). Cychosz et al. (2008) studied a number of MOFs having different pore sizes and shapes for the adsorption of various SCCs in model oils and found that MOFs are superior to other porous adsorbents like zeolites or activated carbon due to the selectivity towards SCCs. Compared to SCCs, very few reports have been published for the adsorptive removal of NCCs with MOFs. Nuzhdin *et al.* (2010) used highly porous chromium terephthalate, MIL-101(Cr) to remove various NCCs from light cycle oil, and a maximum adsorption capacity of 19.6 mg N g^{-1} was reached. They attributed the high nitrogen adsorption capacity to the coordination of the NCCs on the Cr^{3+} sites (CUS) of the MIL-101(Cr)

MOFs provide important features to become a support material for catalyst due to their high surface areas, large pores and porosities. Moreover, some MOFs can be used solely as catalyst for specific reactions. They are promising candidates for catalytic applications. However, the main weakness of MOFs is their lower thermal, hydrothermal and chemical stability for catalysis applications. Some MOF types require a guest solvent residing their pores for utilization. Another drawback of MOFs is as the temperature increases the organic part loses its durability. Lastly, some organic materials used in MOF structure are vulnerable to moisture (Farrusseng *et al.*, 2009).

HKUST-1 is an outstanding demonstration of the concept of Lewis acid MOFs. HKUST-1 was shown to be quite selective, which is typical of hard Lewis acid centers (Lee *et al.*, 2009). Henschel *et al.* (2008) investigated the behavior of MIL-101 as a cyanosilylation catalyst. The results show that as a cyanosilylation catalyst MIL-101 is much more active than HKUST-1. Moreover, the catalytic sites of MIL-101 are immune to unwanted reduction by benzaldehyde in contrast to those of HKUST-1.

The palladium-based catalyst was shown to be active for CO oxidation and cyclooctene hydrogenation. More recently, chemical-based methods were developed to prepare 1 wt% palladium-supported MOF-5 by either incipient wetness impregnation or co-precipitation. Activity superior to Pd/C was observed for the hydrogenation of various alkenes and esters in three-phase reactions (Opelt *et al.*, 2009). Nanosized Au was investigated in various MOF supports such as CPL-1, CPL-2, HKUST-1, MIL-53 and MOF-5. Very narrow gold cluster distribution centered at 1 nm is found for 1 wt % Au/MIL-53(Al). All gold-supported catalysts are active for the aerobic oxidation of benzyl alcohol in methanol. Au/MOF-5 showed the highest catalytic activity for obtaining methyl benzoate, with a yield of 91% at full conversion at 80 °C, whereas copper-based MOFs, which are Lewis acids, drive the selectivity toward benzaldehyde. It is suggested that the MOF support affects the gold cluster so that the activation of alcohol is allowed in the absence of a base, in contrast to active carbons (Ishida *et al.*, 2008).

The characteristic of MIL-53 (Al) is obtained from the literature. It has a BET surface area of 1294 m^2g^{-1}, and a microporous volume is about 0.65 cm^3g^{-1}. Its structure is also durable to water. The thermal stability of the material is high compared to other MOFs. It starts to decompose at 520 °C, which is a high decomposition temperature and suggests that MIL-53 (Al) is a robust framework (Qian *et al.*, 2013). In the study, MIL-53 (Al) is sourced commercially from Sigma-Aldrich under the trademark name Basolite A100. The Basolite A100 has a BET surface area of 1100-1500 m^2g^{-1}, bulk density of 0.4 g cm^{-3} with particle size 31.55 µm.

2.5. Microchannel Reactors

Packed-bed reactors are the most commonly used reactor types in the industry. However, there are some drawbacks of packed reactors, such as mass and heat transfer resistances and complications of scaling up. The idea of microchannel reactor utilization emerged to address aforementioned drawbacks. The structure of a microchannel reactor is comprised of parallel, identical channels with diameters between 10 to several hundred micrometers. This indicates that surface area range is between 10000 and 50000 m^2/m^3 and volume reduction is up to ca. 90% (Ehrfeld *et al.*, 2001). High surface area and compact nature of microchannel reactors ensure high and effective heat transfer rates, which result in to prevent the hot spot formations. Due to its structure, adjustment from laboratory scale to industrial scale is much easier in microchannel reactors. Another advantage of the microchannel reactors is that they provide safe operation while producing highly reactive and hazardous products due to its small dimensions (Commenge *et al.*, 2004). The other benefit of them is its short residence time, which improves the selectivity of the desired products (Ehrfeld *et al.*, 2001). Last of all, mass transfer limitation is overcomed in microchannel reactor due to high mass transfer coefficient at smaller diameters at fully developed laminar flow (Fichtner *et al.*, 2001).

There are several materials of construction of microchannel reactors, such as stainless steel, aluminum alloys, copper, silicon, polymers, ceramic and glass, silver, titanium etc. The selection is based on operating condition of the target system. For adiabatic conditions, material should have low thermal conductivity and high durability. Fabrication methods are determined according to desired substrate. Generally, good thermal and pressure resistance are expected from the material of construction (Watts and Wiles, 2006).

The utilization of microchannel reactors on WGS reaction can be beneficial to surpass the thermodynamic and kinetic limitations. Combining a heat exchanger with microchannel reactor, the reaction system can be maintained at desired temperatures along the reactor. Consequently, two-step process involving LTS and HTS reactions could be turned into single unit process. In addition to this, the system volume is significantly reduced with utilization of microchannel reactors. Therefore, the integration of

microchannel reactors to fuel cell applications becomes very attractive (Baier and Kolb, 2007).

3. EXPERIMENTAL WORK

3.1. Materials

3.1.1. Chemicals

All chemicals used for catalyst preparation are presented in Table 3.1.

Table 3.1. Chemicals used for catalyst preparation.

Chemicals	**Formula**	**Source**	**Molecular Weight (g/mol)**
Gamma alumina	γ-Al_2O_3	Alfa Aesar	101.96
MIL-53(Al)	$C_8H_5AlO_5$	Sigma-Aldrich	208.10
Cerium(III) nitrate hexahydrate	$Ce(NO_3)_3.6H_2O$	Sigma-Aldrich	434.22
Tetraammineplatinum(II) nitrate	$Pt(NH_3)_4(NO_3)_2$ 50.4wt%Pt	Sigma-Aldrich	387.22

3.1.2. Gases and Liquids

All of the gases used in experimental study were supplied from Linde Group, Istanbul. The deionized water is obtained by Zeneer Water Purification System and its conductivity is less than 0.1 $\mu S.cm^{-1}$. Deionized water is used as reactant and in catalyst synthesis. All liquids and gases used in the experimental study are presented in Table 3.2 and Table 3.3 respectively.

Table 3.2. Specifications and applications of the liquids used.

Liquid	Specification	Application
Water	Deionized (DI)	Catalyst Synthesis, Reactant

Table 3.3. Specifications and applications of the gases used.

Gas	Specification (%)	Application
Argon	99.995	GC Carrier Gas
Carbon dioxide	99.995	Reactant, Product
Carbon monoxide	99.999	Reactant, Product
Helium	99.999	GC Carrier Gas
Hydrogen	99.995	Reactant, Product, Reducing Agent
Nitrogen	99.998	Inert

3.2. Experimental Systems

The experimental systems used in the study comprised mainly into three groups:

- Catalyst Preparation Systems: These systems include setups for support preparation and incipient-to-wetness impregnation steps of catalyst preparation.
- Catalyst Characterization System: This system is used for characterizing surface structure of used or reduced catalysts and for measuring the metal percentages inside of catalyst by using Scannic Electron Microscopy (SEM) integrated with Energy Dispersive X-ray Spectroscopy (EDX). To observe the crystal structure X-ray Diffraction (XRD) is utilized.
- Catalytic Reaction System: The system consisted of a feed section including mass flow controllers for inlet gases, HPLC pump for water feed and a furnace for temperature control of the catalyst bed.
- Product Analysis System: The quantitative analysis of the reactant and product streams made by two online gas chromatographs.

3.2.1. Catalyst Preparation Systems

Incipient-to-wetness impregnation technique is utilized to prepare the catalysts in the study. The catalyst preparation system includes a Buchner flask, a vacuum pump for evacuating, a Retsch UR1 ultrasonic mixer for uniform mixing and a Masterflex peristaltic pump for impregnation of active metal. Entire system is demonstrated in Figure 3.1.

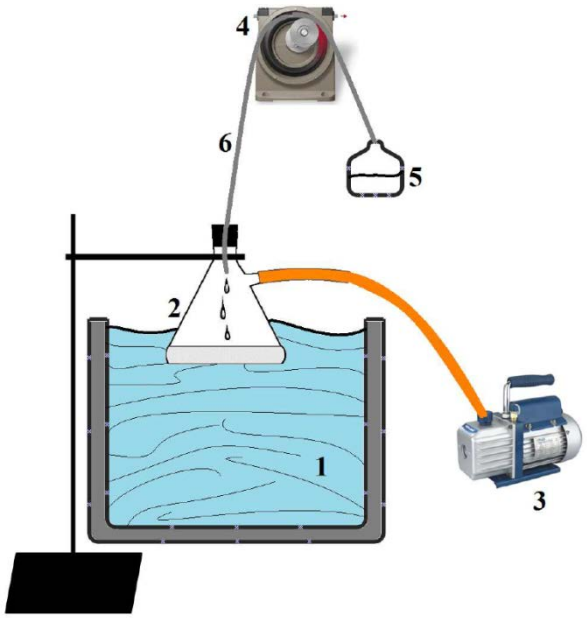

Figure 3.1. The Impregnation System: 1. Ultrasonic Mixer, 2. Buchner Flask, 3. Vacuum Pump, 4. Peristaltic Pump, 5. Aqueous Catalyst Solution, 6. Silicon Tubing (Karakaya, 2012).

3.2.2. Catalyst Characterization System

The structural analysis of the catalyst samples were carried out at Boğaziçi University Advanced Technologies R&D Center through Backscattering Electron-Scanning Electron Microscopy (BSE-SEM) and Energy Dispersive X-ray Analysis (EDX) using a Philips XL30 ESEM-FEG unit, and through X-ray Diffraction (XRD) using a Rigaku D/MAX-Ultima and equipment.

3.2.3. Catalytic Reaction System

The catalytic reaction and analysis system (Karakaya, 2012) comprised of three subsections (Figure 3.2):

- Feed section
- Reaction section
- Product analysis section

In feed section, reactant gases H_2, CO_2, CO and inert N_2 are stored in pressurized storage cylinders and are passed on mass flow controllers (MFCs) by adequate gas regulators. The gases are sent to corresponding MFC independently through 1/8” tubing. The required amount of gases are fed to the downstream via Bronkhorst model F-201CV digital mass flow controllers, whose calibration curves are provided in Appendix A. The downstream is controlled by a three-way valve directing the flow toward either the reaction chamber or gas chromatographs for feed analysis.

The liquid reactant deionized water is pumped to the system by a Shimadzu LC-20AD HPLC pump. The transportation of liquid to the system is provided by 1/16” stainless steels tubing from Swagelok. The liquid is vaporized and kept at 120 °C before the combination of downstream. The temperature of the system is kept at 120 °C from downstream to the entrance of the reactor chamber. The temperature control for vaporization of liquid reactant throughout the system is adjusted with heating tapes and K-type thermocouples with PID temperature controllers.

There is a three-way valve just before the reactor chamber entrance, which is used to send the mixture to the ventilation system or reactor chamber. All reactants are sent to ventilation for 30 minutes before the experiment starts to obtain a uniform mixture of reactants.

In reaction section, the reactant gas mixture enters to 1.0 cm ID x 80 cm quartz reactor, which is located in a furnace. The furnace is controlled by a Shimaden FP23 Programmable Temperature Controller and a K-type sheathed thermocouple. The catalyst

is presented in the middle of the reactor and the thermocouple is coiled up on the reactor starting from the catalyst bed. The exit stream of the reactor is sent to ice cold trap to prevent the undesired damage on gas chromatograph because it is sensitive to liquid water. A Dewar flask is used to sustain the temperature of the cold trap for separation of unreacted water from rest of the gases. After the cold trap, remaining gas is sent over the gas chromatographs for analysis.

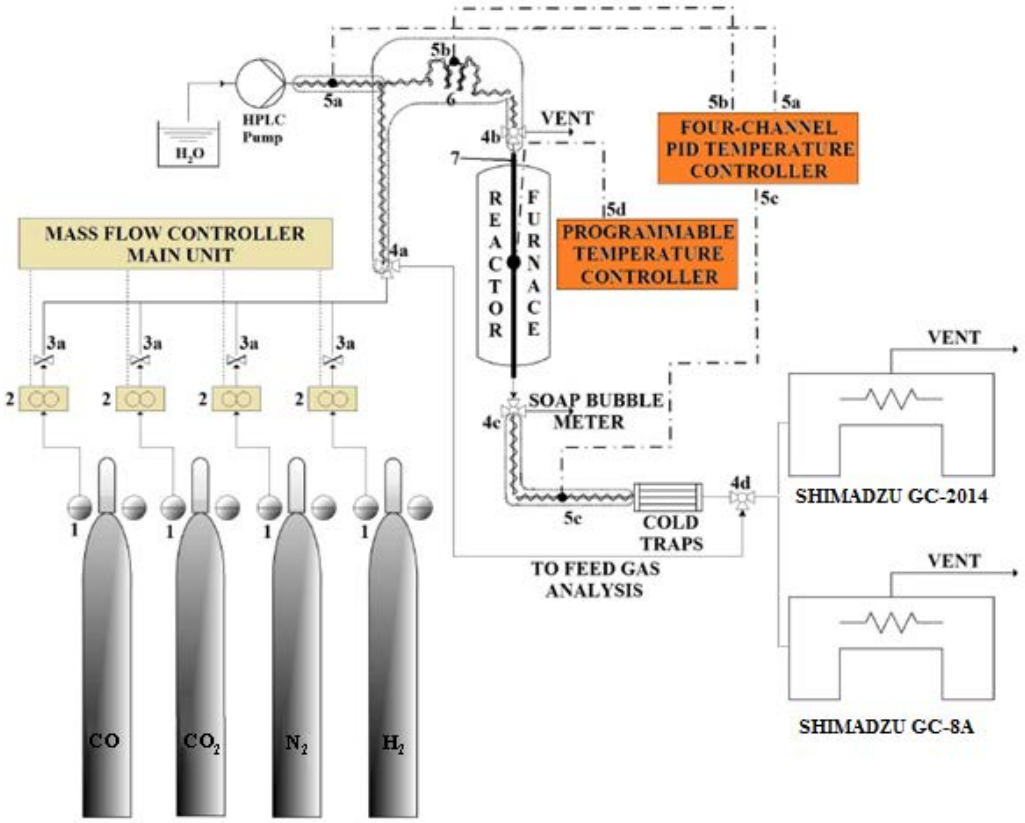

Figure 3.2. Schematic Representation of the Reaction System. 1. Gas Regulators, 2. Mass Flow Controllers, 3. On-O_ Valves, 4. Three-Way Valves, 5. Thermocouple Locations, 6. Mixing Zone, 7. Quartz Tube (Karakaya, 2012).

In product analysis section, the stream coming from the ice trap is sent to two different GCs with a three-way valve. The extensive description is given in Section 3.2.3.

3.2.3. Product Analysis System

The product stream analysis is carried out on dry basis by two different GC's. Shimadzu GC-2014 performs the analysis on a Carboxen 1000 packed column which

detects H_2, N_2, CO_2 and CO. On the other hand, Shimadzu GC-8A contains a Porapak-Q column which detects N_2, CO_2. Shimadzu GC-8A is used to inspect the CO_2 amount in the product feed extensively. Detector of both GCs is thermal conductivity detectors (TCD). Gas chromatograph working parameters are summarized in Table 3.4.

The stream coming from the cold trap is fed continuously to Shimadzu GC-8A and analyzed primarily. After the analysis, the flow is sent to the Shimadzu GC-2014 for two minutes. The analysis is carried out after two minutes and the flow is sent to GC-8A for next sampling. Both GC's sampling loop is 1 Nml.

Before the experiments, calibrations of both gas chromatographs are done by feeding gas mixtures, whose composition is known and set by mass flow controllers, to the GCs. In the chromatographs, each gas forms a unique peak at a specific retention time and the areas under these peaks are provided by GC software. These areas indicate the percentage of the corresponding gas in the analyzed mixture. The calibration curve for each gas is constructed as area versus percentage accordingly and is presented in Appendix B.

Table 3.4. Gas analysis conditions for product gas stream.

	GC-2014	**GC 8A**
Carrier gas	Argon	Helium
Carrier gas flow rate	30 $ml.min^{-1}$	25 $ml.min^{-1}$
Column length x ID	6 m x 3 mm	1.5 m x 3 mm
Column temperature	40 °C (0 →13.5 min) 40 →150 °C (13.5 →15.5 min) 150 °C (15.5→27.5 min)	90 °C (12 min)
Column tubing material	Stainless steel	Stainless steel
Column packing material	Carboxen 1000	Porapak Q
Detector current	50 µA	120µA
Detector type	TCD	TCD
Detector temperature	175 °C	150 °C
Injector temperature	110 °C	90 °C
Sample loop volume	1 ml	1 ml
Gases analyzed	H_2, N_2, CO_2, CO	N_2, CO_2

3.3. Catalyst Preparation and Pretreatment

3.3.1. Catalyst Preparation

In the thesis 1.5 wt% Pt/MIL-53(Al) and 1.5 wt% Pt–5 wt% CeO_2/Al_2O_3 are prepared for the parametric study. Both catalysts are prepared by the incipient-to-wetness impregnation method. However, preparation of 1.5 wt% Pt–5 wt% CeO_2/Al_2O_3 requires sequential impregnation. In addition, the catalyst 1.5 wt% Pt–5 wt% CeO_2/Al_2O_3 is prepared for both packed bed reactor and micro channel reactor due to the requirement of different particle size of the support for the reactor type.

In the first part of the studies, 1.5 wt% Pt/MIL-53(Al) is prepared. The support MIL-53(Al) has the required particle size, which is $32.5x10^{-6}$ m; therefore no support preparation is needed. The support is initially dried at 150 °C for 1 hour in vacuum furnace for removal of humid. Then, it is placed inside a Buchner flask, which is connected on Retsch UR1 ultrasonic mixer. The support is mixed with constant vibration for 30 min under vacuum conditions for opening the pores of the support. In the meantime, 0.030 gr of tetraamineplatinum (II) nitrate is added to 1.7 ml of deionized water for 1 gram of support. The solution is impregnated to the support by using a Masterflex peristaltic pump with a flow rate of 0.5 Nml/min. As a result, the support is completely wetted by impregnation, and the catalyst slurry is kept under vacuum condition and ultrasonically mixing for 90 min to obtain uniform dispersion of metal particles over support. Afterwards, the catalyst slurry is dried for 16 hours at 115 °C in a furnace for removal of water from impregnation. Lastly, the dried catalyst slurry is first crushed to smaller particle size, and then is calcined at 300 °C for 3 hours. The final form of catalyst is stored in a desiccator for further utilization.

The sequential impregnation is utilized for the preparation of 1.5 wt% Pt – 5 wt% CeO_2/Al_2O_3 catalyst. For conventional packed configuration, 250-354 μm (45-60 mesh) particle size γ- Al_2O_3 is utilized. Pellet form γ- Al_2O_3 support material is crushed and sieved to the desired mesh size. On the other hand, 3 micron size of γ- Al_2O_3 is used as the support material for micro coat and micro packed configurations. After support is brought the desired conditions, it is dried at 150 °C for 1 hour in vacuum furnace and placed inside

a Buchner flask, which is connected on Retsch UR1 ultrasonic mixer. The support is mixed for 30 min under vacuum condition. The metal solution is prepared by using 0.135 gr of cerium(III) nitrate hexahydrate and 1.8 ml of deionized water for 1 gram of support. The solution is first mixed and is impregnated to the support via a Masterflex peristaltic pump with a flow rate of 0.5 Nml/min. The resulting slurry is mixed for 90 min in vacuum condition and is dried for 16 hours at 115 °C in a furnace. The dried catalyst is crushed before calcination and it is calcined for 3 hours at 300 °C in a furnace. Afterwards, cooled ceria impregnated alumina is placed inside a Buchner flask, and connected to the ultrasonic mixer and mixed for 30 min at vacuum conditions. The metal solution is prepared by using 0.053 gr of tetraamineplatinum (II) nitrate is added to 1.8 ml of deionized water for 1 gram of support. The solution is mixed and is impregnated to the support via a Masterflex peristaltic pump with a flow rate of 0.5 Nml/min. The platinum impregnated ceria alumina is mixed 90 min and is dried for 16 hours at 115 °C in a furnace. It is crushed and the calcined for 3 hours at 300 °C in a furnace. The final form of catalyst is stored in a desiccator for further utilization.

3.3.2. Catalyst Coating on Microchannel Plates

The activity of 1.5 wt% Pt – 5 wt% CeO_2/Al_2O_3 catalyst is also investigated on micro channel structure. The micro structured reactor is comprised of 310-grade stainless steel single channel cylindrical housing with diameter of 18.6 mm and length of 30 mm and FeCrAlY plates with dimensions of 2 mm x 5 mm x 20 mm, which are inserted into stainless steel housing.

The catalyst preparation is the same as explained in the previous section. Before coating the catalyst, FeCrAlY plates are require a pre-treatment. Plates are calcined at 900 °C for 3 hours in a muffle furnace, which ensures the formation of a native alumina layer on the plates. This layer increases the adhesion of the catalyst coating. Then, the $Pt/CeO_2/Al_2O_3$ catalyst in powder form is wetted by deionized water until a slurry mixture is obtained. The slurry mixture is uniformly coated on 5 mm x 20 mm plates. In the study, it is observed that the coated catalyst amount is between 15 to 20 mg. The coated plates are dried at 115 °C for 16 hours and they are calcined at 300 °C for 3 hours. Last of all, the plates are inserted into the previously cleaned and dried housing. In order to prevent the

displacement of the plate in the housing, certain amount of ceramic wool is inserted at the bottom of the housing. At the end of the preparation, single rectangular microchannel with dimensions 0.75 mm (H) x 4 mm (W) x 20 mm (L) is obtained.

3.4. Reaction Tests

3.4.1. Blank Tests

Blank tests are performed to ensure that the material of construction, glass-wool and δ-alumina have no catalytic activity. The results indicated that these items remain inactive under the reaction conditions.

3.4.2. WGS in Packed Bed Reactor

The packed reactor system is demonstrated in Figure 3.3. In the configuration, glass wool is inserted to the middle of the reactor to prevent the loss of catalyst. The particulate catalyst is, then, poured through the glass wool via a funnel. A K-type thermocouple is wrapped around the reactor and fastened to the reactor. The reactor inner diameter is

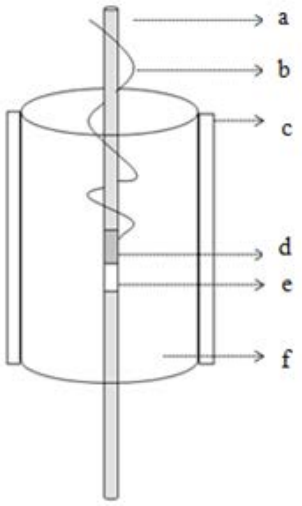

Figure 3.3. Schematic Diagram of the Packed Bed Reactor and Furnace System: a. Reactor b. Thermocouple c. Ceramic Wool Insulation d. Catalyst bed e. Glass Wool f. Furnace. (Ertem, 2014).

10 mm for packed reactor configuration.

The operating conditions for packed reactor configuration are tabulated in Table 3.5. Different feed compositions are investigated through the study, and they are entitled as cases. The detailed information about cases is introduced in Table 3.6. In this configuration, $Pt/CeO_2/Al_2O_3$, Pt/MOF and only MOF catalysts are investigated.

Table 3.5. Operating conditions for WGS reaction in the study for packed configuration.

Operating Parameter	**Parameter value**
Catalyst Amount (mg)	100
Catalyst Particle Size	45-60 mesh (Al_2O_3) $32.5x10^{-6}$ m (MIL-53 (Al)
Reduction Temperature (°C)	350
Reaction Temperature (°C)	250, 300, 325
Reaction Total Flow Rate (Nml/min)	80
W/F Ratio (mg.min/ml)	1.25

Table 3.6. Feed conditions for WGS reaction in the study.

Case Number	**CO (Nml/min)**	**H_2O (Nml/min)**	**CO_2 (Nml/min)**	**H_2 (Nml/min)**	**Total Flow Rate (Nml/min)**
1	10	30	10	20	80
2	10	30	15	15	80
3	10	30	20	10	80

Experimental results are reported in terms of the conversion of CO with respect to feed concentration, which is defined in Equation 3.1:

$$CO\ Conversion\ \% = \frac{C_{CO}^{in} - C_{CO}^{out}}{C_{CO}^{in}} x100 \tag{3.1}$$

The experimental road map for packed configuration is given in Table 3.7.

Table 3.7. Experimental road map for WGS reaction in the study for packed configuration.

Case	Catalyst	Temperature (°C)
1	MIL-53 (Al)	300
	1.5 wt% Pt/MIL-53 (Al)	250
		300
		325
	1.5 wt%Pt – 5 wt% CeO_2/Al_2O_3	250
		300
		325
2	MIL-53 (Al)	300
	1.5 wt% Pt/MIL-53 (Al)	250
		300
		325
	1.5 wt%Pt – 5 wt% CeO_2/Al_2O_3	250
		300
		325
3	MIL-53 (Al)	300
	1.5 wt% Pt/MIL-53 (Al)	250
		300
		325
	1.5 wt%Pt – 5 wt% CeO_2/Al_2O_3	250
		300
		325

3.4.3. WGS in Microchannel Reactor

Microchannel reactor experiments can be divided two sub-sections, namely micro coated and micro packed reactor. In micro coated configuration (Figure 3.4a), 1.5 wt% Pt – 5 wt% CeO_2/Al_2O_3 catalyst is utilized, in which the support particle size is 3 microns. The experiments are conducted by using quartz tube with an inner diameter of 20 mm, single plate steel housing and one FeCrAlY plate. Housing with plate is embedded in the middle of the quartz tube and supported underneath by hollow ring, which is demonstrated in Figure 3.4b. Temperature of the reaction is regulated by K-type thermocouple, which is wrapped around the quartz tube.

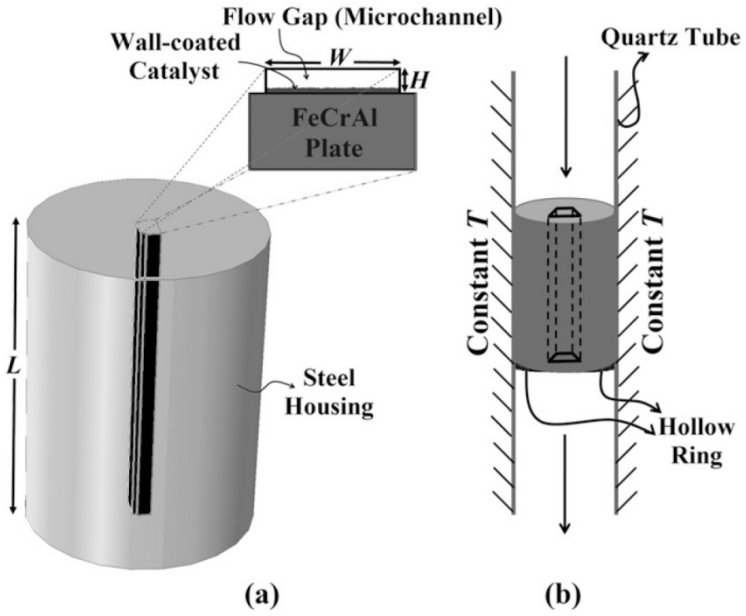

Figure 3.4. Coated Microchannel Reactor Configuration. a. Coated microchannel reactor b. Location of steel housing in quartz tube (Karakaya *et al*., 2012).

In micro packed configuration, same catalyst is used as in micro coated configuration. The catalyst is diluted with alumina in this configuration. The experiments are conducted by using quartz tube with an inner diameter of 20 mm, two-channel steel housing and one FeCrAlY plate. The demonstration of micro packed reactor is given in Figure 3.5.

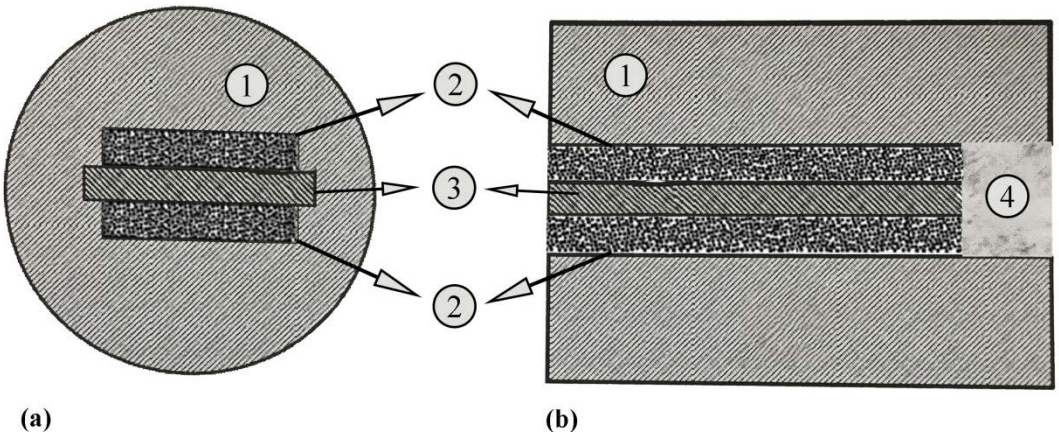

Figure 3.5. Packed Microchannel Reactor. a. Top view b. Cross-sectional view. (1: Stainless steel housing; 2: Packed microchannels; 3: FeCrAlY; 4: Ceramic wool plug).

The investigation of feed composition is carried out according to the plan presented in Table 3.6. Moreover, one experiment in absence of H_2 and CO_2 is conducted at 300 °C and entitled as ideal case in the results. In ideal case, CO and H_2O flow rates are kept at 10 and 30 Nml/min, which are same with cases given in Table 3.6. N_2 amount is determined as 40 Nml/min to keep the total flow constant. The effect of temperature is examined for two temperatures. All necessary experimentation data for micro packed configuration are tabulated in in Table 3.8.

Table 3.8. Operating conditions for WGS reaction in the study for micro packed configurations.

Operating Parameter	**Parameter value**
Catalyst Amount (mg)	15
Catalyst Particle Size (micron)	3
Dilution Amount (mg)	30
Reduction Temperature (°C)	300
Reaction Temperature (°C)	250, 300
Reaction Total Flow Rate (Nml/min)	80
W/F Ratio (mg.min/ml)	0.19

Table 3.9. Experimental road map for WGS reaction in the study for micro packed configuration.

Case	**Catalyst**	**Temperature (°C)**
Ideal	1.5 wt% Pt – 5 wt% CeO_2/Al_2O_3	300
1		250
		300
2		250
		300
3		250
		300

The results obtained from micro channel configuration are aimed to be compared with the packed configuration. However, due to the narrow space in microchannel system, employable amount of catalyst is limited in micro configuration. This situation restrains the comparison between two configurations due to different W/F ratios. Therefore, all experiments conducted in micro packed configuration are repeated with packed configuration according to Table 3.8. The experiment list is given in Table 3.9.

3.4.4. WGS in 2 mm ID Quartz Reactor

In this configuration, effect of reactor diameter is investigated. The reactor utilized in these tests is similar to packed reactor configuration, which has a 10 mm ID along the reactor. However, this reactor has a 2 mm region in the middle of reactor, where catalyst is packed. The reactor has 80 cm height and the glass wool is placed center of the reactor, then, required amount of catalyst is added to the reactor. The schematic representation of the reactor system is demonstrated in Figure 3.6.

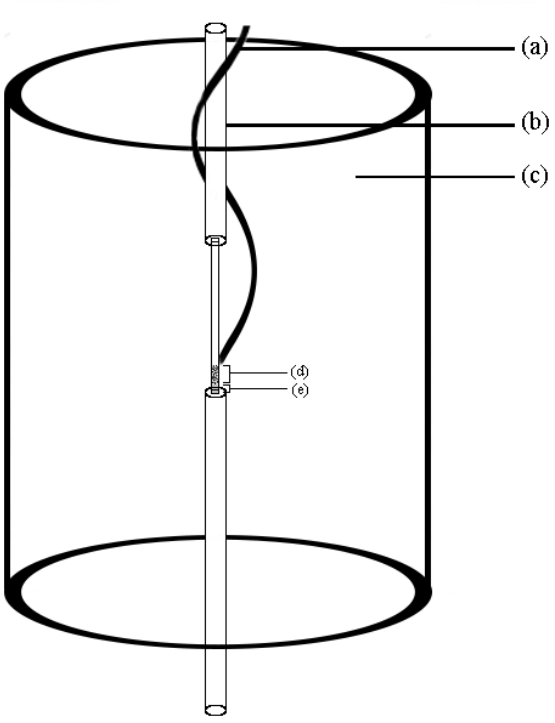

Figure 3.6. Schematic Diagram of the 2 mm ID Packed Bed Reactor and Furnace System: a. Thermocouple b. Reactor c. Furnace d. Catalyst e. Glass Wool.

Due to the narrow spacing in this configuration, experiments conducted in Section 3.4.2 could not be repeated in this setup to investigate the effect of reactor diameter. New road map is constituted to investigate the effect of reactor. The operating conditions and experimental road map is given in Table 3.10 and 3.11 respectively. The selection for operating conditions is based on similar to micro packed investigation. The reason is that parametric investigation for $Pt/CeO_2/Al_2O_3$ for 3 micron support size for packed configuration is already performed. This situation, therefore, enables to investigate the effect of particle size on CO conversion. The effect of feed composition also investigated according to Table 3.6.

Table 3.10. Operating conditions for WGS reaction in the study for 2 mm ID Quartz Reactor.

Operating Parameter	**Parameter value**
Catalyst Amount (mg)	15
Catalyst Particle Size (mesh)	45-60
Dilution Amount (mg)	30
Reduction Temperature (°C)	300
Reaction Temperature (°C)	250, 300
Reaction Total Flow Rate (Nml/min)	80
W/F Ratio (mg.min/ml)	0.19

Table 3.11. Experimental road map for WGS reaction in the study for 2 mm ID Quartz Reactor.

Case	**Catalyst**	**Temperature (°C)**
1	1.5 wt% Pt – 5 wt% CeO_2/Al_2O_3	250
		300
2		250
		300
3		250
		300

To sum up, the effect of reactor configuration is investigated 2 mm ID and 10 mm ID quartz reactors for 45-60 mesh size $Pt/CeO_2/Al_2O_3$, whereas the effect of particle size is examined using the results from this part and previous section for 10 mm ID quartz reactor.

4. RESULTS AND DISCUSSIONS

The study presents the results of a parametric study on WGS reaction and is divided into several sections. In the first section, catalytic performance of $Pt/CeO_2/Al_2O_3$ is investigated for different feed compositions and temperatures. The second section involves the results of the experiments involving MIL-53 (Al) supported catalysts. The performance of Pt/MIL-53(Al) is investigated at the same conditions with $Pt/CeO_2/Al_2O_3$ for comparison purposes. In the third section, the effect of reactor configuration is investigated in the context of microchannel and packed reactor configurations. In the fourth section, effects of reactor diameter and catalyst particle size are examined. The last section contains catalyst characterization results from XRD over fresh and used catalyst and SEM/EDX analyses for different particle sized catalysts.

4.1. WGS Reaction over $Pt/CeO_2/Al_2O_3$ for Packed Configuration

In the section, investigation of $Pt/CeO_2/Al_2O_3$ catalyst on WGS reaction is studied at different temperatures, namely 250, 300 and 325 °C. The catalyst of interest is 1.5 wt% of Pt, 5 wt% of CeO_2 and rest is alumina. Particle size of the catalyst is between $2.50x10^{-1}$ to $3.54x10^{-1}$ mm, corresponding to 45 to 60 mesh size. The experiments are conducted in a 10 mm ID tubular quartz reactor with 100 mg catalyst. Effect of feed composition is also investigated; the tested feed compositions are tabulated in Table 3.6 and entitled as case in the following figures. The investigation of feed conditions is carried out at constant S/C ratio of 3 and N_2 amount of 10 Nml/min, whereas H_2 and CO_2 amounts are varied according to the plan presented in Table 3.6. Total flow rate is kept constant during all experiments at 80 Nml/min.

The theoretical equilibrium compositions are determined by HSC Chemistry software, in which the Gibbs Free Energy Minimization method is utilized. Theoretical CO conversions are then calculated using the theoretical equilibrium compositions and they are presented together with their experimental counterparts. The experimental conversions are obtained by 5 hours of experimentation. During the experiments, it is observed that catalytic activity decreases with time in the first 2 hours, after which it reaches to a steady-

state value. Therefore, the reported conversions are determined by taking the average of data between 2 and 5 hours.

In Figure 4.1, effect of temperature for each feed composition is demonstrated. It is observed that CO conversion increases with temperature. The reason is that WGS becomes kinetically favorable with temperature, and Pt atoms present more active behavior at temperatures of 300 °C and above (Wheeler *et al.*, 2004). The low conversions at 250 °C and major conversion difference between 250 and 300 °C can also be explained by the activity of Pt atoms. The temperature increase magnifies the H_2 production in all cases. On the other hand, theoretical CO conversion decreases with temperature. This result is expected since WGS reaction is an exothermic and reversible reaction. Although the theoretical conversion decreases, it is still higher than 90 %. It is observed that the closest point to equilibrium conversion is attained at 325 °C for all cases. The closest experimental conversion to theoretical one is achieved for Case 3 at 325 °C.

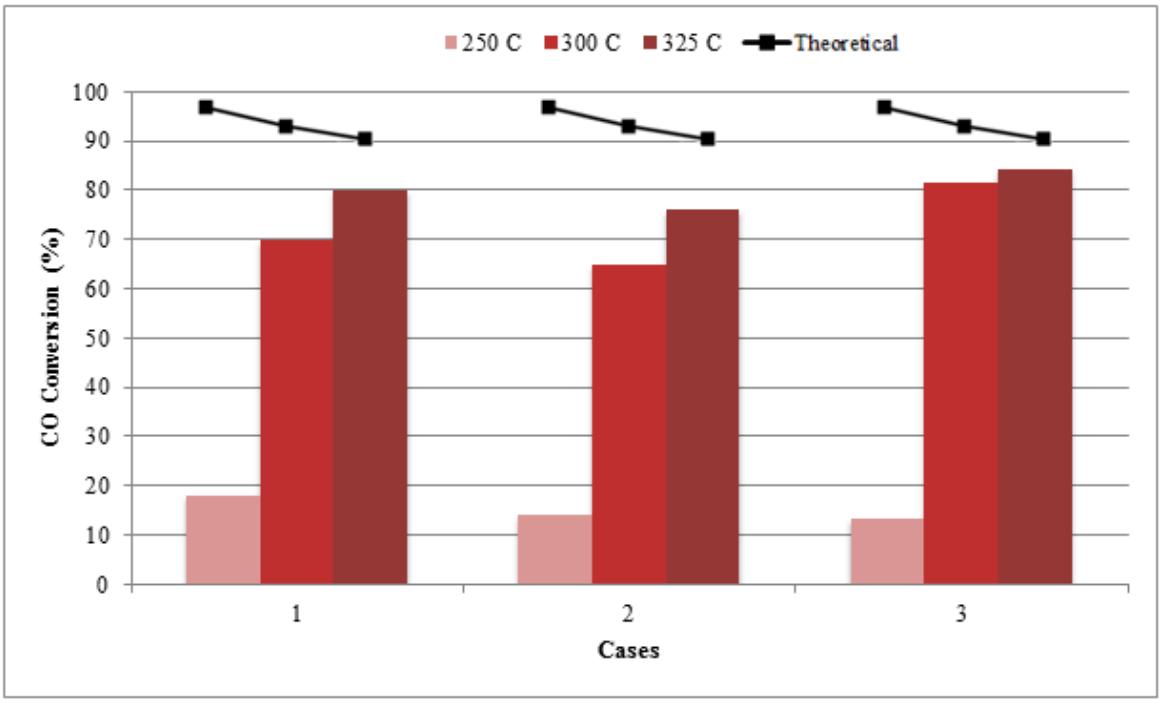

Figure 4.1. Results for Effect of Temperature on CO Conversion for All Cases over 1.5 wt % Pt –5 wt% CeO_2 / Al_2O_3.

The effect of feed composition is demonstrated in Figure 4.2. First of all, theoretical conversions are examined, and it is observed that they are equal for Cases 1 and 3, whereas the theoretical conversion is lower for Case 2 with respect to other cases. Since WGS is an equilibrium reaction, its extent is a function of equilibrium constant, which depends only on temperature. Change in composition of reactants in Cases 1, 2 and 3 does not shift the equilibrium constant. However, since the equilibrium constant is comprised of multiplication of partial pressures of products divided by partial pressures of reactants, change in amount of product affects the amount of the reactants. As a result, higher value at numerator in Case 2 result in a higher value in denominator to keep the equilibrium constant fixed. Therefore, with increased amount of CO result in a lower conversion at Case 2 with respect to Cases 1 and 3.

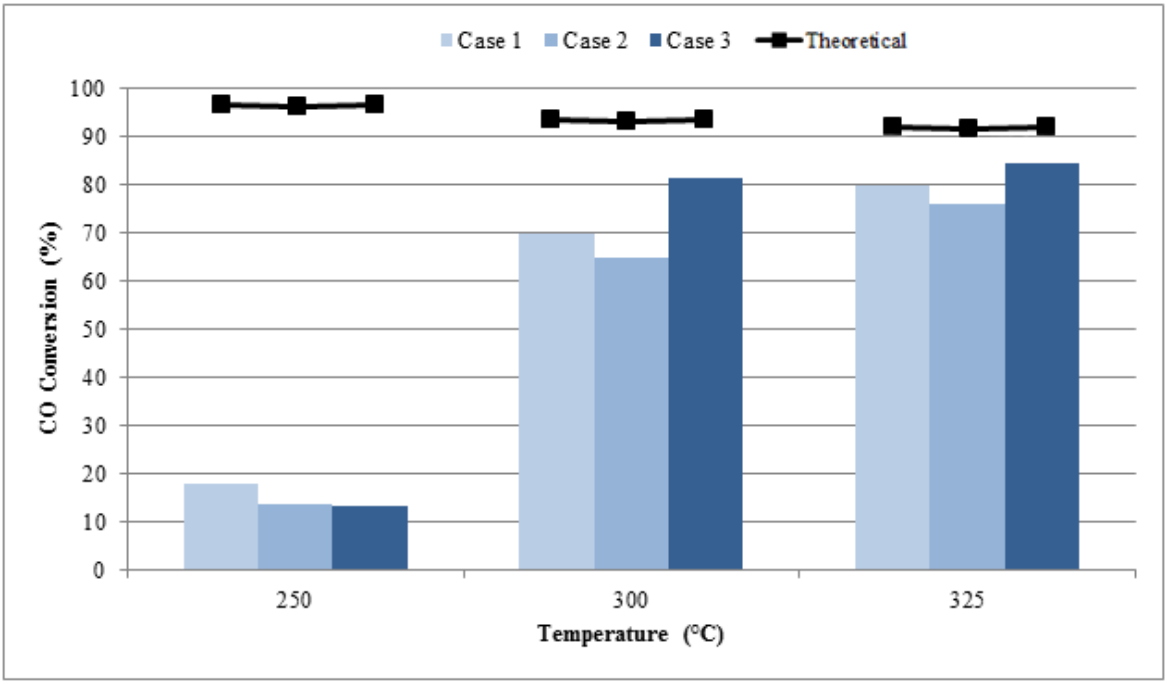

Figure 4.2. Results for Effect of Feed Composition on CO Conversion for All Temperatures over 1.5 wt % Pt –5 wt% CeO_2 / Al_2O_3.

In experimental results, it is observed that experimental results for Case 2 are in accordance with the theoretical outcomes except the outcomes obtained at 250 °C. The experimental conversion at 250 °C for Case 3 is lower than the conversion of Case 2, which can be caused by inactivity of Pt atoms. Another reason can be related to the fact

that the ceria's oxygen vacancies may not distributed adequately, which result in low performance at given experiment.

It is expected that experimental conversions of Case 1 and 3 are equal with respect to theoretical results; however, there is a significant difference between them. The possible reason for this difference can be caused by the activity of ceria, which promotes Pt activity in WGS reaction by its oxygen storing and releasing behavior. The more ceria stores the oxygen, the more Pt activity increases due to the interaction between CO atoms on Pt atoms and O_2 atoms on ceria. In Case 3, the amount of CO_2 in the feed is higher than that involved in Case 1. In presence of higher amounts of oxygen atoms, ceria may have been stored higher amounts of oxygen, which concluded the high performance of Case 3 with respect to Case 2. Amount of oxygen presence in the feed increases the H_2 production accordingly. All results are tabulated in Table 4.1.

Table 4.1. Conversions for Packed Configuration over $Pt/CeO_2/Al_2O_3$.

Case #	**Catalyst**	**Temperature (°C)**	**Experimental Conversion (%)**	**Theoretical Conversion (%)**
1	1.5 wt % Pt – 5 wt% CeO_2 / Al_2O_3	250	18.0	96.8
		300	69.8	93.2
		325	80.0	90.7
2		250	13.8	96.6
		300	64.9	92.9
		325	75.9	90.4
3		250	13.3	96.8
		300	81.4	93.2
		325	84.2	90.7

4.2. WGS Reaction over Pt/MIL-53(Al) for Packed Configuration

This section presents investigation of Pt/MIL-53(Al) catalyst on WGS reaction in packed reactor configuration for comparison with the previous section. The study carried out at different temperatures, namely 250, 300 and 325 °C. The catalyst is composed of 1.0

wt% of Pt and rest is MIL-53(Al). The experiments conducted in a 10 mm ID tubular quartz reactor with 100 mg catalyst. Effect of feed composition is also investigated and the tested feed compositions are tabulated in Table 3.6. The investigation of feed conditions is carried out at constant S/C ratio of 3 and N_2 amount of 10 Nml/min, whereas H_2 and CO_2 amounts are varied according to the plan presented in Table 3.6. Total flow rate is kept constant during all experiments at 80 Nml/min. Total flow rate is kept constant during all experiments at 80 Nml/min.

In the first part of the experimentation, effect of MIL-53(Al) on CO conversion investigated. In these trials, only MIL-53(Al) is used as the catalyst and investigation is carried out for each case at 300 °C. The results show that there is no CO conversion in the presence of MIL-53(Al). After this result, parametric study over 1 wt% Pt/MIL-53(Al) is carried out. The results are given in Figures 4.3 and 4.4, for effect of temperature and effect of feed composition respectively.

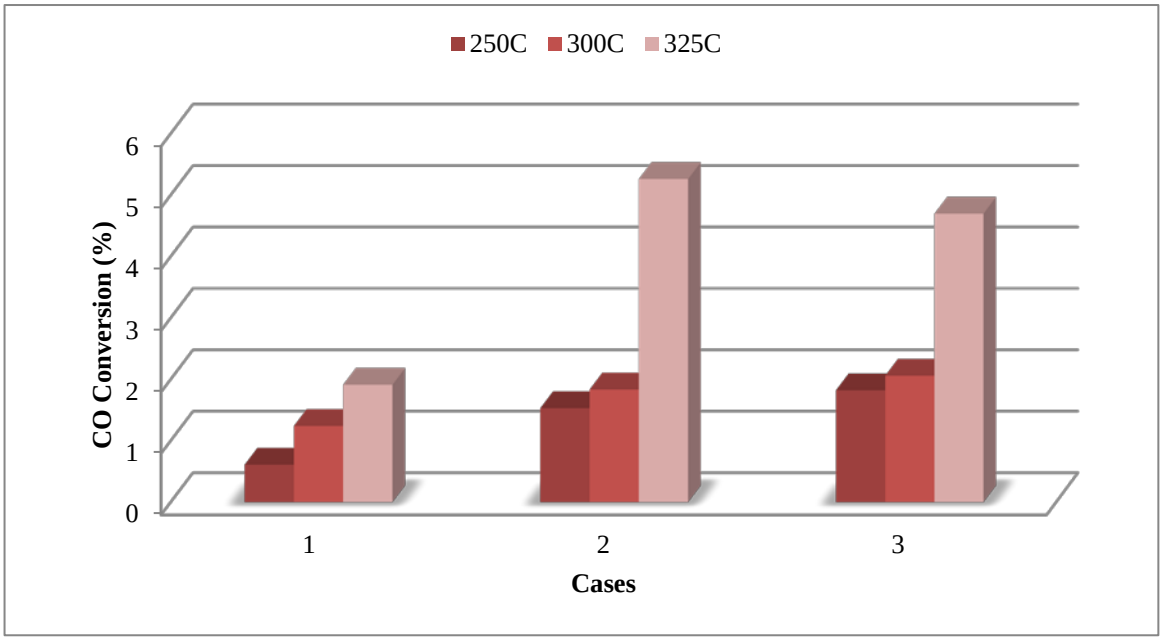

Figure 4.3. Results for Effect of Temperature on CO Conversion for All Cases over 1 wt.% Pt/MIL-53(Al).

In Figure 4.3, it is observed that the conversion for each case increases with temperature due to the favorable kinetic environment for the WGS. However, conversions

are quite low and in the effect of feed composition analyses, the conversion trends are not in the expected form. In order to understand the reasons behind these outcomes, structural analysis of MIL-53(Al) is carried out via X-Ray Diffraction (XRD) method. The XRD analysis is performed for two MIL-53(Al) samples. First sample is previously ordered for another study in our group and is used for catalyst preparation in my study, which provided low conversions. On the other hand, the second sample is ordered fresh for comparison purposes. For further discussion, they are referred as old and fresh MIL-53(Al) respectively. The results are provided in Section 4.4. It is observed that the crystal structure of old MIL-53(Al) is considerably changed with respect to fresh sample. The main reason for the change in crystal structure can be linked to the sensitivity of the MIL-53(Al) against the storage conditions such as humidity, which can affect the organic part of the MIL-53(Al). It is concluded that the storage conditions are quite important for MIL-53(Al).

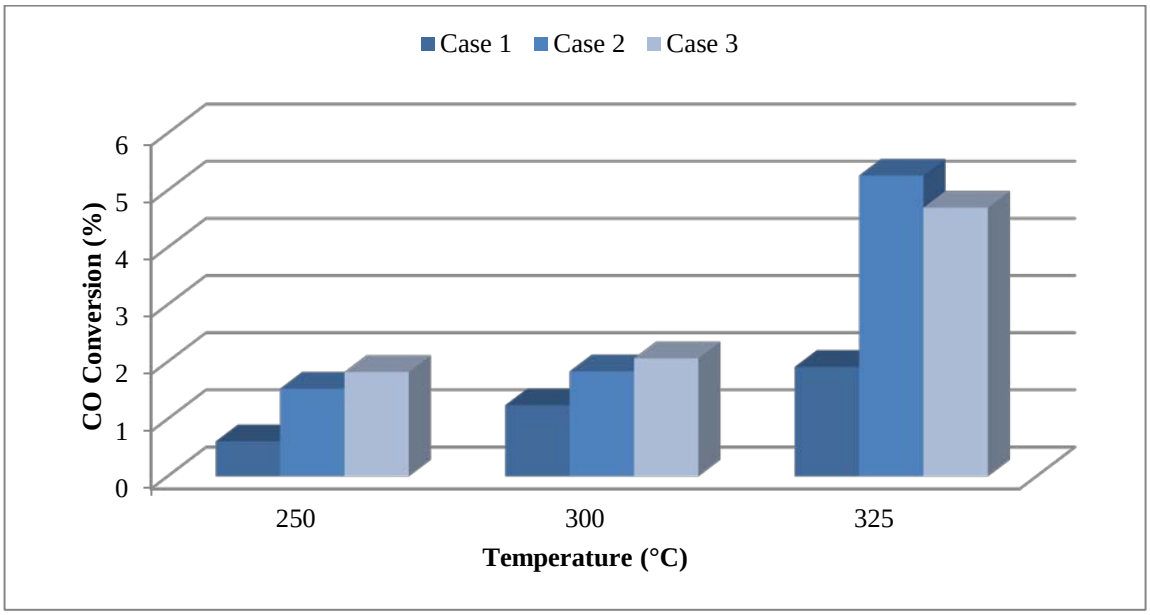

Figure 4.4. Results for Effect of Feed Composition on CO Conversion for All Temperatures over 1 wt.% Pt/MIL-53(Al).

The parametric study is proceeded with Pt/MOF catalyst including fresh MIL-53(Al), and the Pt weight percentage is defined as 1.5 %. Several experiments are conducted with new catalyst; however, the activity was lower than old Pt/MIL-53(Al) catalyst. Another XRD analysis is carried out new Pt/MIL-53(Al) catalyst and compared with that of the fresh MIL-53(Al). The difference in crystal structures of two samples is found to be

significant. The detailed results for XRD analysis is given in Section 4.4. The results indicate that incipient-to-wetness impregnation method for catalyst preparation is not suitable for MIL-53(Al). The possible reason for change in crystal structure is the sensitive nature of MOF's organic part to the water. The results of parametric study of 1 wt. % Pt/MIL-53(Al) on WGS reaction are given in Table 4.2.

Table 4.2. Conversions for Packed Configuration over Pt/MIL-53(Al).

	Temperature (°C)	**CO Conversion (%)**
Case 1	250	0.61
	300	1.24
	325	1.91
Case 2	250	1.53
	300	1.83
	325	3.26
Case 3	250	1.82
	300	5.26
	325	4.70

4.3. WGS Reaction over $Pt/CeO_2/Al_2O_3$ for Microchannel Configurations

In this section, effect of reactor configuration on CO conversion is investigated. $Pt/CeO_2/Al_2O_3$ catalyst is used in the experiments. Particle size of the catalyst is defined as $3x10^{-3}$ mm, which is smaller than those used in packed reactor configuration due to the narrow space in microchannel. The necessary information about conducted test parameters and operation information is provided in Section 3.4.3.

At the first stage of the experimentation, micro coated microchannel configuration is studied. The catalyst preparation and coating procedure are introduced in Sections 3.3.1 and 3.3.2 respectively. The final form of coated catalyst on FeCrAlY plate is demonstrated in Figure 4.5a. The experiments are conducted by using a quartz tube with an inner diameter of 20 mm, single plate steel housing and one FeCrAlY plate. This configuration is tested for ideal feed composition rate at 300 °C. At the end of the experiment, it is

observed that the coated catalyst is fallen off from the plate surface. In order to understand the reason of falling, several trials are conducted. First of all, the effect of flow rate is investigated on different coated plates with N_2 amounts of 50 and 80 Nml/min. It is concluded that falling is not positively correlated with the flow rate. The second investigated parameter is the effect of presence of steam. Different steam flow rates are examined, such as 10, 20 and 30 Nml/min. However, at each trial the catalyst is fallen off from the surfaces, which are demonstrated in Figure 4.5b. According to the literature, water molecules adsorbed to the ceria atoms on the catalyst surface and disassociate to hydrogen and oxygen on the ceria atoms (Azzam *et al.*, 2008).The water affinity of the ceria might have caused the catalyst loss from the surface of the plate. Moreover, Goerke *et al.* (2004) suggested that ceria supported catalyst stick weakly on plates. Therefore, it is concluded that the utilization of ceria on coating on FeCrAlY plates is not suitable, even though it is a promoter, i.e. not the actual support of the catalyst.

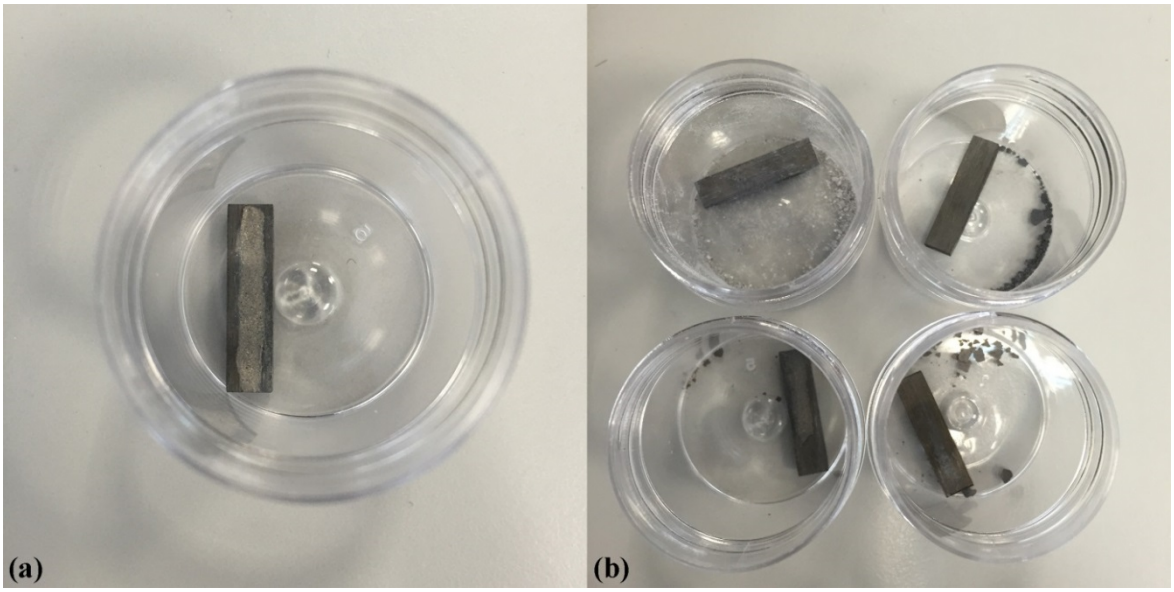

Figure 4.5. FeCrAlY plates. a. Catalyst coated (before testing) b. Catalyst fallen off (after testing).

The investigation of micro reactor configuration is proceeded with the micro packed reactor configuration. Before the experimentation, the packing capacity of a single microchannel is determined as 25 mg of $Pt/CeO_2/Al_2O_3$. However, this amount of catalyst is not applicable to packed reactor because the required catalyst height for plug flow

condition, which is the ratio of the bed height to particle diameter should exceed 50, is not achieved. Therefore, as a solution, dilution with alumina is implemented to attain the plug flow condition. Different dilution ratios are studied, and it is concluded that as the amount of diluent alumina increases in catalyst-support mixture, the CO conversion increases. The possible reasons of this outcome are that alumina can provide a more isothermal environment for reaction, and it can favor more uniform distribution over the reactive flow over the catalyst particles. After the trials, the most suitable catalyst-to-diluent ratio is selected as 0.5 and catalyst and diluent amounts are determined as 15 mg and 30 mg, respectively. The designated amount of catalyst-support mixture is suitable for packed reactor configuration; however, 45 mg mixture is improper for micro packed reactor utilization in a single channel. Therefore, two-channel micro reactor configuration (Figure 3.5) is utilized and the total amount of catalyst-support mixture is divided equally for each channel.

The experimentation started with ideal gas composition at 250 °C, in which no catalytic activity was observed. The possible reasons are that the Pt sites are not active properly at the experiment temperature and the catalyst amount is quite low, which also affects the catalytic activity. Last of all, due to the allowance between the metal housing and quartz reactor, some of the flow can pass through the vacancy between the housing and the reactor. After ideal gas composition trial, new trials are carried on at 300 °C with Cases 1, 2 and 3. It is found that CO conversions are lower than 3 %. These low CO conversions indicate that channeling between housing and reactor has high impact on catalytic activity in this configuration.

The last part of this investigation involves testing packed reactor configuration with $3x10^{-3}$ mm $Pt/CeO_2/Al_2O_3$ at different feed compositions. The first trial is carried out at 250 °C and no catalytic activity is observed due to the aforementioned reasons. The experiments at 300 °C are examined and the results are demonstrated in Figure 4.6.

As expected, the highest conversion is obtained for ideal feed composition case. Due to the thermodynamic constraints involved in WGS the absence of product gases favors the forward reaction, and, hence CO conversion. In presence of product gases, the highest conversion is obtained for Case 3. The reason for this outcome can be the increased

activity of the CeO_2 due to the abundance of CO_2 in the feed. On the other hand, the lowest conversion is obtained for Case 2. The feed composition of Case 2 leads to higher numerator value in equilibrium constant, which indicates a higher denominator part. Since the CO is presented in the denominator, lower CO conversion is observed with respect to Cases 2 and 3. All experimental CO conversion results are tabulated in Table 4.3.

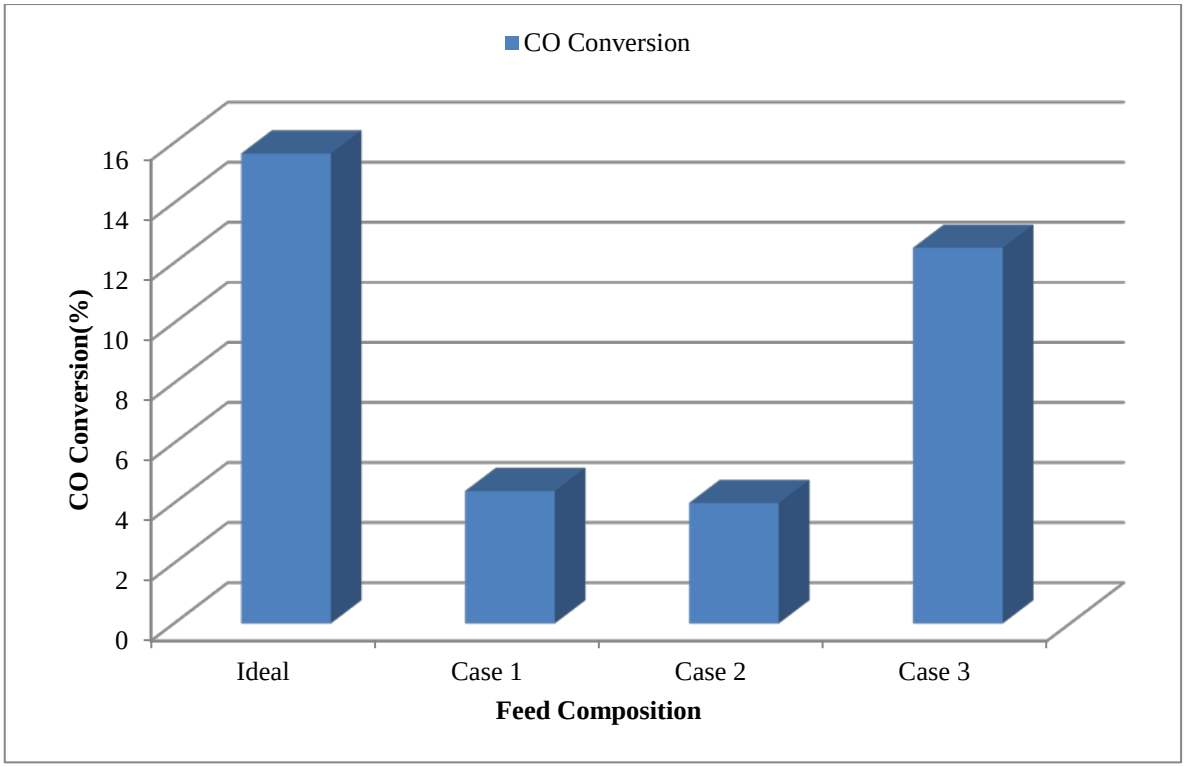

Figure 4.6. Results for Effect of Feed Composition on CO Conversion at 300 °C for 3-micron $Pt/CeO_2/Al_2O_3$ Packed Reactor Configuration.

Table 4.3. Conversions for Packed Reactor Configuration over 3-micron $Pt/CeO_2/Al_2O_3$ at 300 °C.

Case #	Catalyst	CO Conversion (%)
Ideal	3-micron 1.5 wt% Pt – 5 wt% CeO_2/Al_2O_3	15.64
1		4.4
2		4
3		12.5

4.4. Investigation of Reactor and Catalyst Configuration on WGS Reaction over $Pt/CeO_2/Al_2O_3$

In the section, effects of reactor diameter and catalyst particle size on CO conversion are investigated. The 45-60 mesh size ($3.02x10^{-3}$ mm average particle diameter) $Pt/CeO_2/Al_2O_3$ catalyst is utilized to investigate the effect of reactor diameter for two tubular reactors with different internal diameters, namely 2 mm and 10 mm. Moreover, the effect of catalyst particle size is examined by utilization of results for $3x10^{-3}$ mm $Pt/CeO_2/Al_2O_3$ catalyst for packed reactor configuration at Section 4.3 and results for 45-60 mesh $Pt/CeO_2/Al_2O_3$ for 10 mm ID quartz reactor from this section.

The experiments are carried out in presence of product gases, and feed composition for trials are given in Table 3.6. The parametric study started with the trials at 250 °C, in which there was no activity. Then, it is proceeded with the experiments at 300 °C. The results and comparison are demonstrated in Figure 4.7.

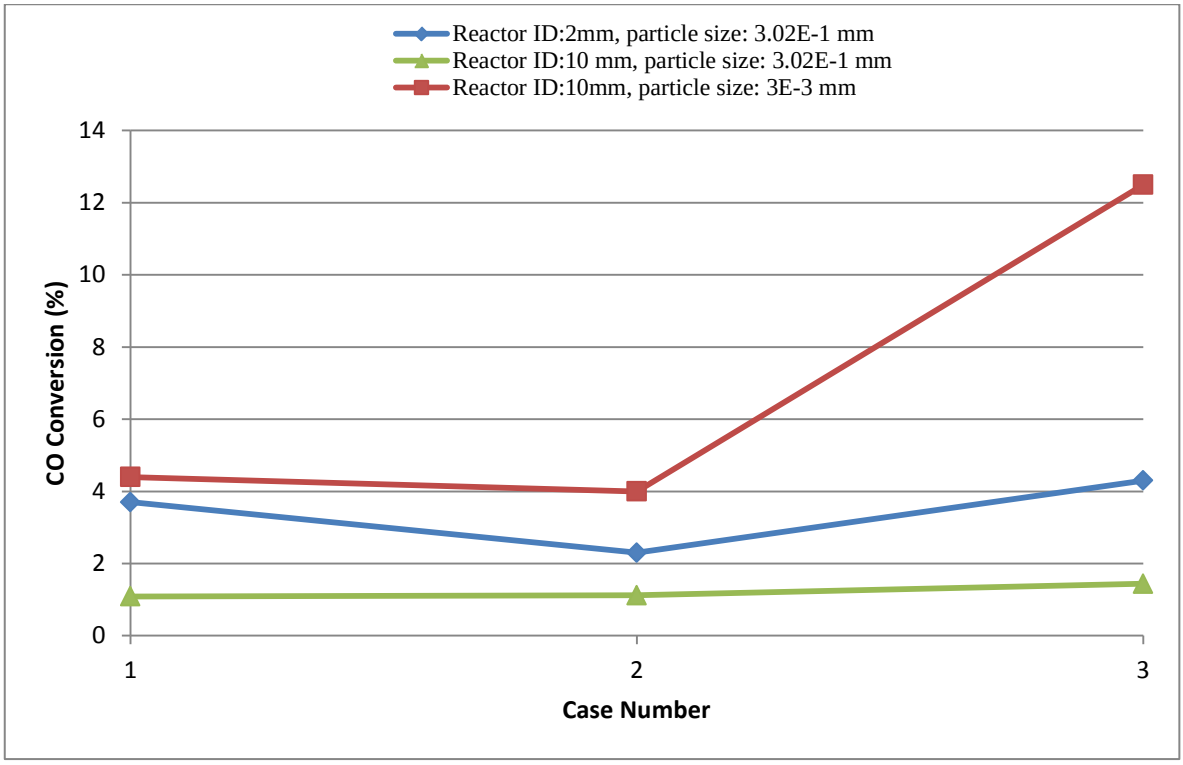

Figure 4.7. Results for Effect of Reactor Inside Diameter and Catalyst Particle Size on CO Conversion over WGS Reaction.

In Figure 4.7, it is observed that conversion trends through the cases are similar to previous sections expect the trials conducted in 10 mm ID packed reactor over catalyst with $3.02x10^{-3}$ mm average particle size. Since the conversion levels are low, the accuracy of the results is expected to be low. Therefore, the difference for this set is neglected.

When the effect of reactor diameter is investigated, it is observed that as the diameter of the reactor decreases, CO conversion increases. As the diameter decreases, the superficial velocity increases; therefore, the Reynolds number increases. With the increased Reynolds number, the mixing in the catalyst bed is promoted. Consequently, the interaction between molecules and catalyst increases, which result in increase in CO conversion.

Table 4.4. Conversions for Different Packed Reactor Configurations over $Pt/CeO_2/Al_2O_3$ catalyst.

Case #	**Reactor ID**	**Catalyst size**	**CO Conversion (%)**
1	2 mm	45 – 60 (mesh)	3.70
			2.30
			4.30
2	10 mm	45 – 60 (mesh)	1.09
			1.12
			1.44
3	10 mm	$3x10^{-3}$ mm	4.40
			4.00
			12.5

The investigation for effect of catalyst particle size shows that as the particle size decreases, CO conversion increases. As the particle size decreases, pore depth can be decreased, and the intraparticle mass transfer resistance can be suppressed. Moreover, smaller particle size indicates higher surface area, which also has a positive effect on CO conversion. There is a major conversion difference between $3x10^{-3}$ mm and 45-60 mesh sized particles for 10 mm reactor at Case 3. In addition to aforementioned reasons, in 3-

micron catalyst, bigger molecules such as CO_2 can easily contact with the active centers. It is previously stated that the presence of CO_2 can promote activity of ceria. Consequently, CO conversion increases as the CO_2 molecules more easily contact with the catalyst. All results for investigation of reactor and catalyst configurations are tabulated in Table 4.4.

4.5. Catalyst Characterization

4.5.1. XRD Results

As mentioned before, unexpected conversion outcomes obtained over MOF-supported catalysts called for the investigation of the crystal structure of MIL-53 (Al). The investigation is carried out between old MIL-53 (Al) and fresh MIL-53 (Al) in the first subsection. The effect of impregnation of Pt on MIL-53 (Al) is examined in the second subsection.

4.5.1.1. MIL-53 (Al). Untreated samples that are neither used for experimentation nor exposed to reduction are employed in XRD characterization. The analyses are carrid out on two samples of MIL-53(Al). One of the samples, named as the old sample, was obtained from supplier (Sigma-Aldrich) in 2014, while the other one, obtained in March 2015, is named as fresh sample for further discussion. In Figure 4.6, the XRD analysis for fresh MIL-53 (Al) is demonstrated, whereas the comparison between old and fresh samples is given in Figure 4.7. It is observed that there are major changes in two-theta peaks. The peak at 8 two-theta changed completely, whereas the 12, 18, 25 and 27 two-theta peaks are extended. The peaks at 33 and 42 two-theta become more apparent. It is concluded that MIL-53 (Al) is degenerated over time. Serre *et al.* (2002) reported that MIL-53 (Al) adsorbs atmospheric water immediately at room temperature. It is possible that although the material kept under careful preservation, it is affected during usage period.

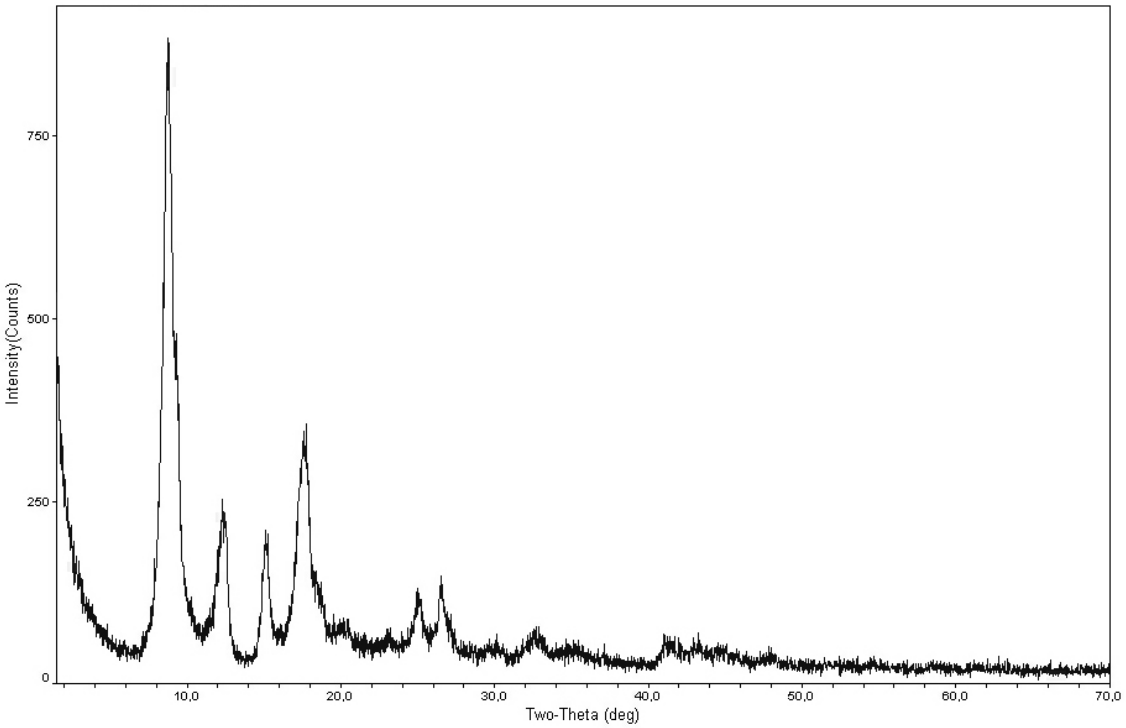

Figure 4.8. XRD Result for Fresh Untreated MIL-53(Al).

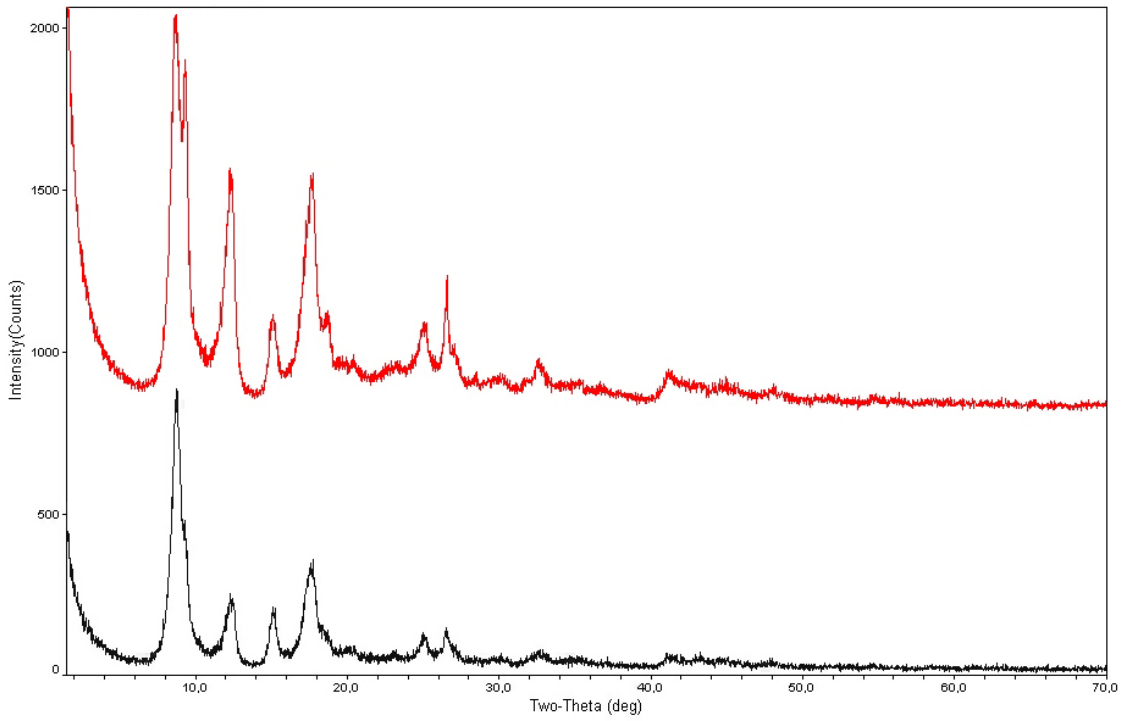

Figure 4.9. XRD Results for Old Untreated MIL-53(Al) (red) and Fresh Untreated MIL-53(Al) (black).

4.5.1.2. 1.5 wt% Pt/MIL-53 (Al). In order to explore the possible cause of low catalytic activity, XRD analyses are conducted for unused and Pt impregnated MIL-53 (Al). The XRD result for Pt impregnated MIL-53 (Al) is given in Figure 4.8; whereas the comparison of crystal structures between unused and Pt/MIL-53 (Al) is introduced in Figure 4.9. It is observed that there are major changes in 8, 12, 18 and 25 two-theta peaks, which indicated the crystal structure is degenerated after the impregnation of Pt.

The nature of the MOF materials is sensitive to moisture and liquid water. The susceptibility of MIL-53 (Al) has already been tested under water vapor at different temperatures and it was found out that the material is stable at 350 °C at 50 % humid conditions (Low *et al.*, 2009). During catalyst preparation deionized water is utilized in incipient-to-wetness method, which might have affected the organic structure of the MIL-53 (Al). As a result, it is concluded that another catalyst preparation method rather than incipient-to-wetness method should be taken into consideration for future work.

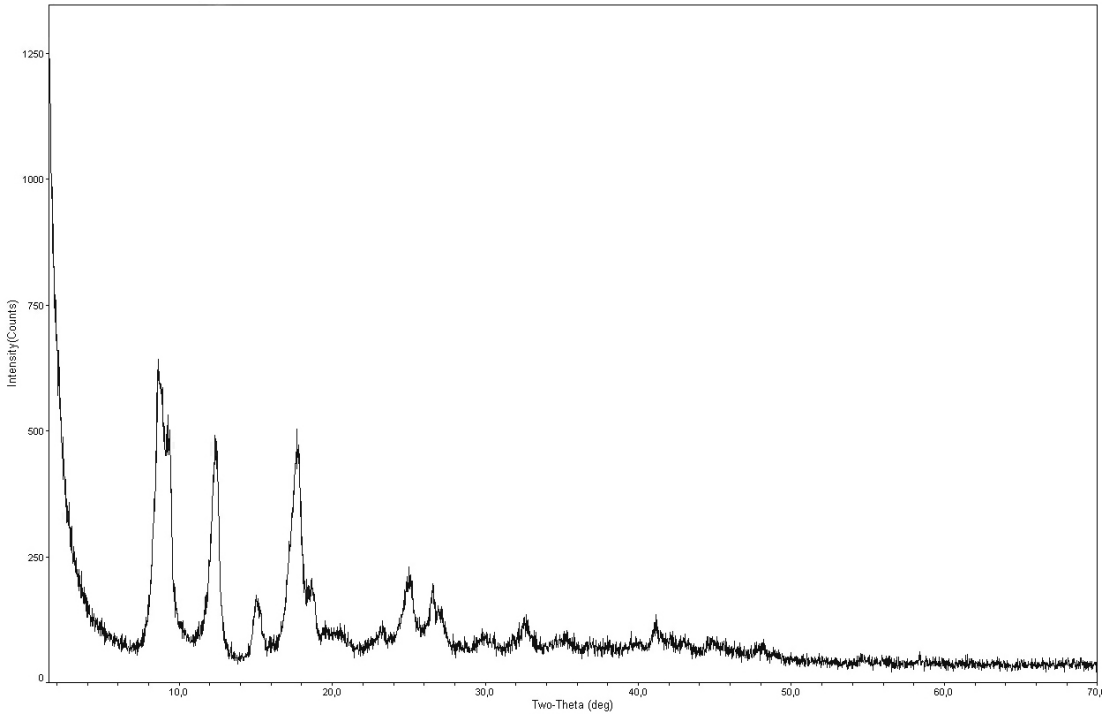

Figure 4.10. XRD Result for Unused1.5 wt% Pt/MIL-53(Al) Catalyst.

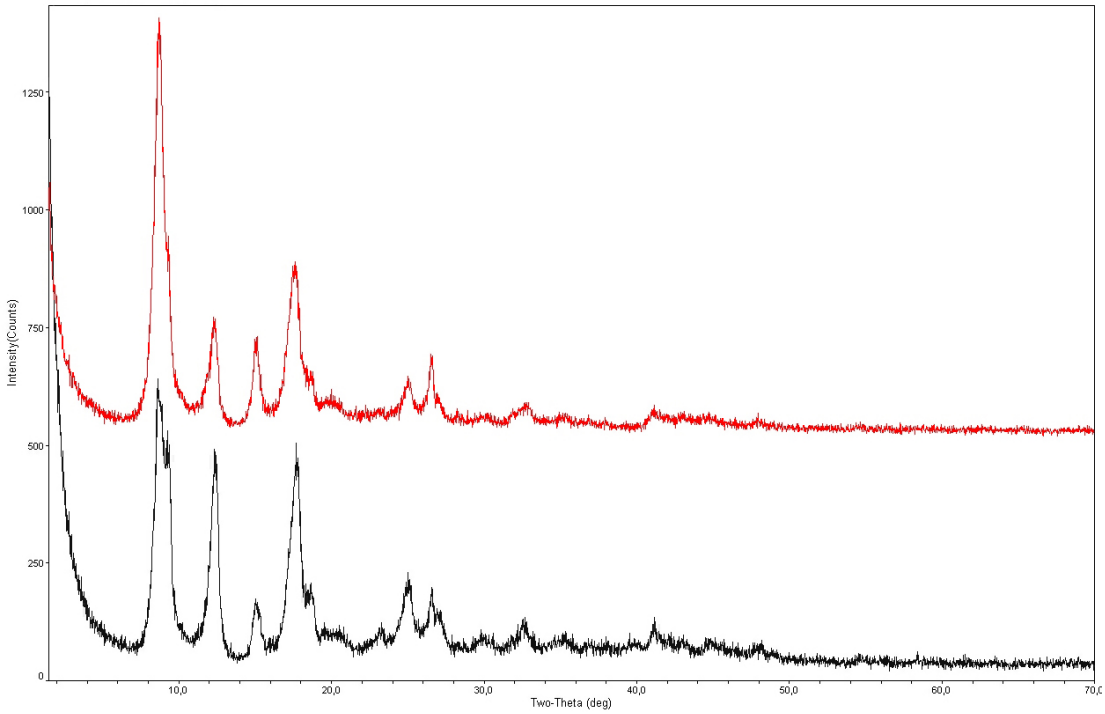

Figure 4.11. XRD Results for Untreated MIL-53(Al) (red) and Unused1.5 wt% Pt/MIL-53(Al) Catalyst (black).

4.5.2. SEM/EDX Results

Scanning Electron Microscopy (SEM) and Energy Dispersive X-Ray Spectroscopy (EDX) surface characterization methods are carried out for freshly reduced and used $Pt/CeO_2/Al_2O_3$. The investigation is conducted for two different catalyst particle sizes, namely $3x10^{-3}$ and $3.02x10^{-1}$ mm average particle sized catalyst, to find out possible reasons for outcomes obtained in Section 4.4. Moreover, one spent 45-60 mesh sized catalyst sample is utilized for SEM analysis to understand whether there is coke formation or agglomeration on the catalyst after utilization. Last of all, metal mapping studies are performed to understand the dispersion of metals and whether the agglomeration of metals occurs on the support surface during reaction.

In Figure 4.12, SEM image for freshly reduced $3x10^{-3}$ mm $Pt/CeO_2/Al_2O_3$ catalyst is demonstrated. It is observed that Pt sites, observed as bright spots, are well dispersed over the support. In Figure 4.13a, presence of the Pt atoms are apparent with bright dots. Due to the issues in the light source of the SEM machine, magnification is limited to 10000x;

therefore, better imagining on $3x10^{-3}$ mm particles cannot be performed. The presence of Pt atoms could not be seen in Figure 4.13b, however, when the mapping analysis is carried out for the image, well dispersed Pt atoms are observed.

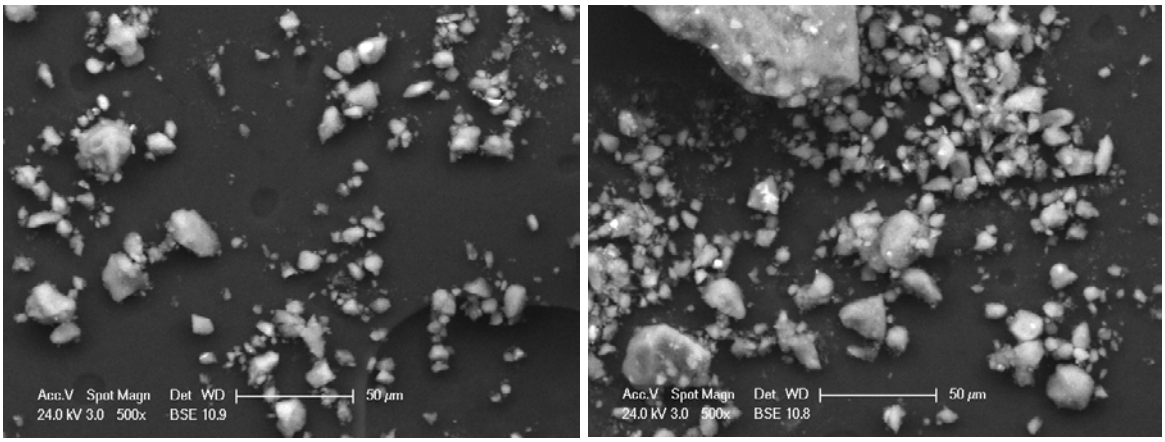

Figure 4.12. SEM image for freshly reduced 3-micron sized 1.5 wt % Pt–5 wt% CeO_2/Al_2O_3 catalyst (500x).

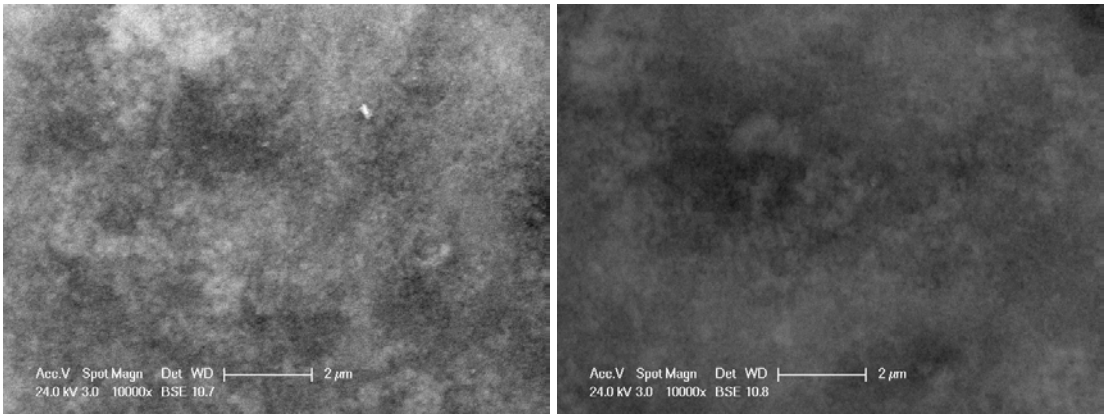

(a) (b)

Figure 4.13. SEM image for freshly reduced 3-micron sized 1.5 wt % Pt–5 wt% CeO_2/Al_2O_3 catalyst (10000x).

In Figure 4.14, results of metal mapping study are given. It is observed that the Ce and Pt atoms are very good disturbed over the catalyst surface except one little point in which density of Pt atoms are very high. This outcome may be caused by the incipient-to-wetness catalyst preparation method. During the impregnation, it is possible to coincide some of Pt atoms on the same surface.

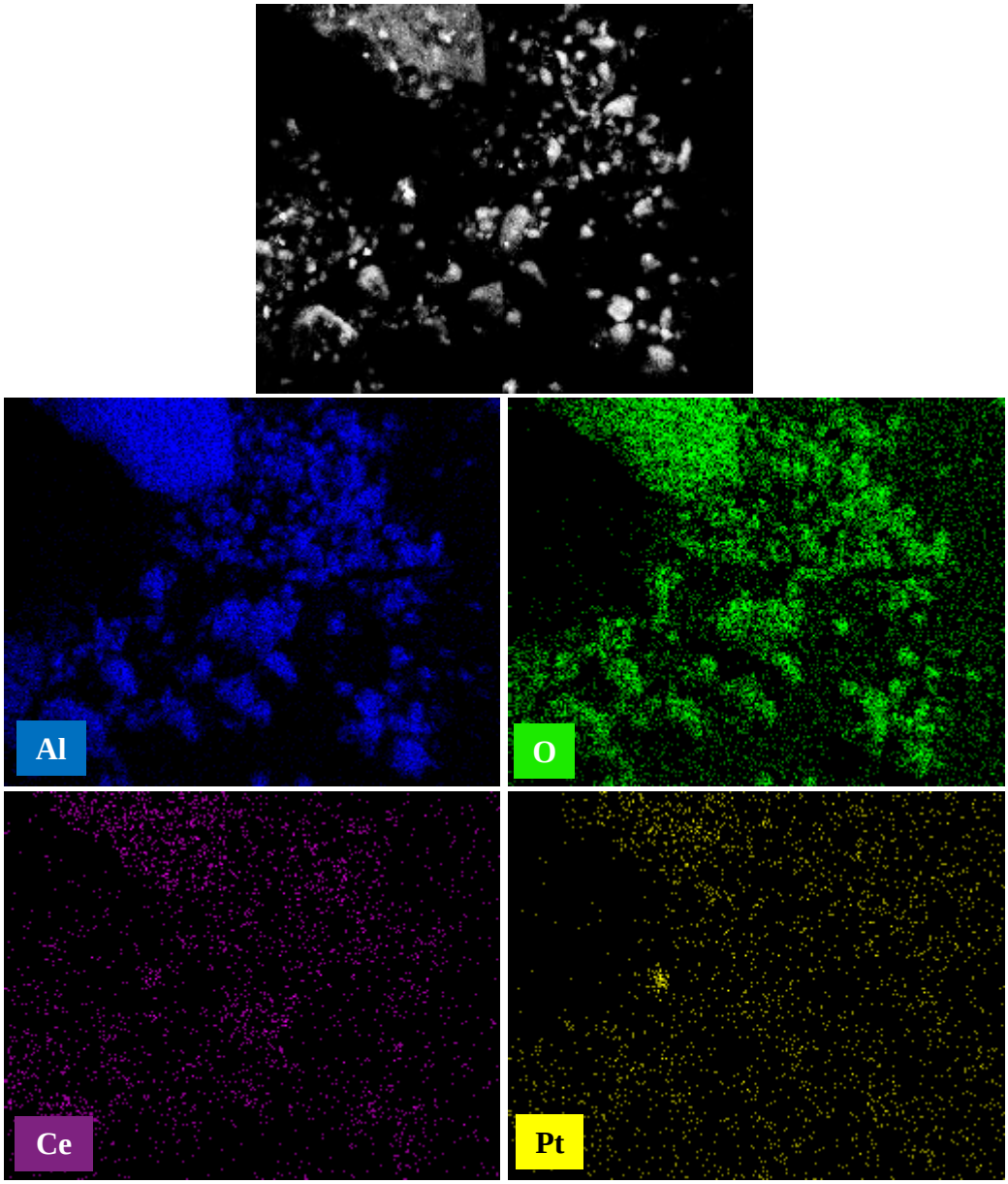

Figure 4.14. Mapping of freshly reduced 3-micron sized 1.5 wt % Pt–5 wt% CeO_2/Al_2O_3 catalyst.

In Figure 4.15, the SEM image for freshly reduced 45-60 mesh sized 1.5 wt % Pt–5 wt% CeO_2/Al_2O_3 catalyst is showed with 50x magnification. It is observed that the catalyst particle size is in desired range. Some of the Pt atoms are gathered together on the same particle, which a very bright particle with respect to other particles. In Figure 4.16, it is observed that the porous structure of Al_2O_3 and some of Pt particles, which are bright dots on the picture. Since the Al_2O_3 is not a suitable material for SEM analysis system, pictures does not have good quality.

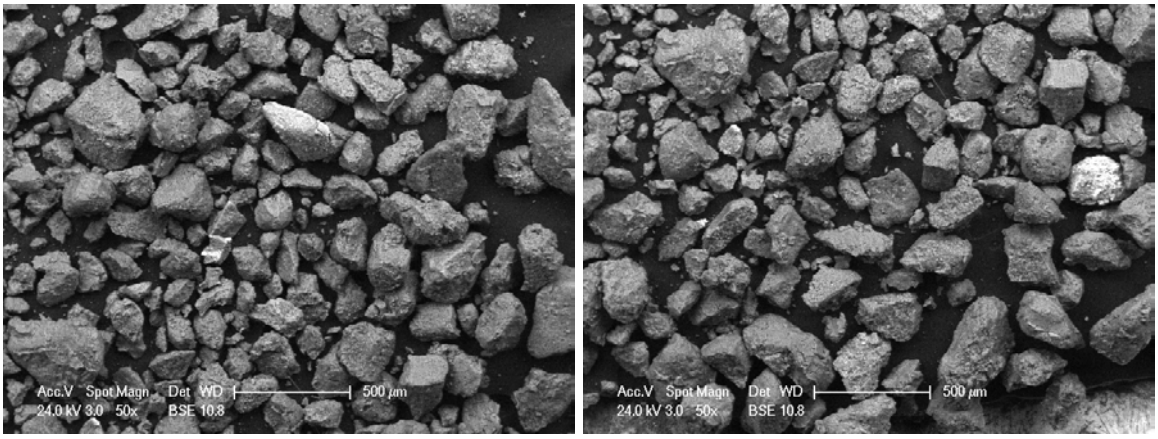

Figure 4.15. SEM image for freshly reduced 0.3 mm particle sized 1.5 wt % Pt–5 wt% CeO_2/Al_2O_3 catalyst (50x).

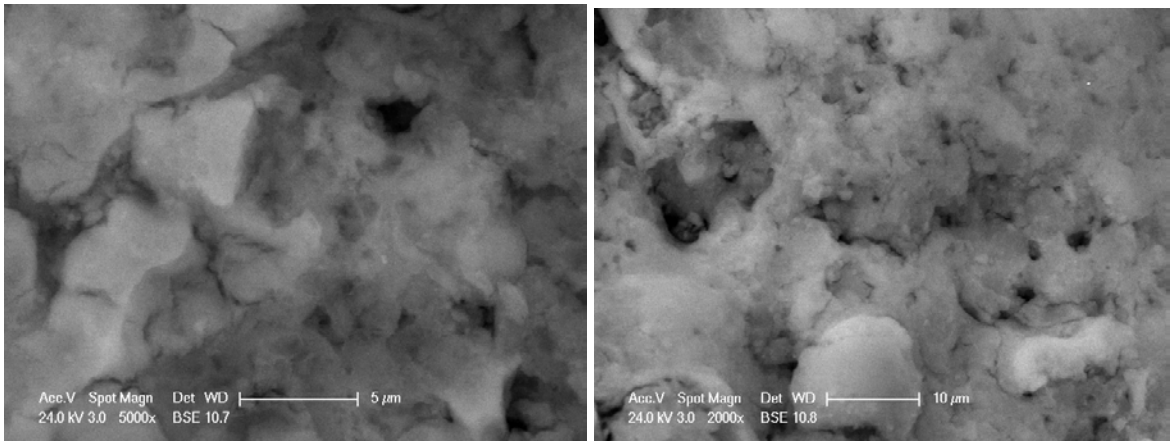

(a) (b)

Figure 4.16. SEM image for freshly reduced 0.3 mm particle sized 1.5 wt % Pt–5 wt% CeO_2/Al_2O_3 catalyst a. Magnified 5000x b. Magnified 2000x.

The Figures 4.17 and 4.18 provide SEM analysis results for the spent 1.5 wt % Pt–5 wt% CeO_2/Al_2O_3 catalyst. Comparison of Figures 4.15 and 4.17 show that no carbon formation occurred upon the reaction. This outcome is supported by the EDX analyses (not shown here) which do not indicate the presence of carbon on the spent samples. EDX analysis also show that metal loadings are suitable for Ce atoms around 5.5 wt%, however, for Pt atoms it is above the expected value. The obtained Pt loadings are in range between 2.5 to 3 wt %, which can be caused from the accuracy of the analysis system. Under 2 wt

% loadings, the system does not provide accurate results, therefore, this outcome is not taken into consideration. SEM analysis also show that porous structure of the catalyst is un affected by the reduction and reaction conditions (Figures 4.16a and 4.18a). When the Figure 4.18b is examined, big white spots are observed on the surface. In order to understand whether these points indicate agglomeration or not, EDX mapping is carried out. Outcomes of this study (not shown here) indicate the Pt atoms are well dispersed over the surface and the image provided in Figure 4.18b view is caused by the poor imaging from the analysis equipment.

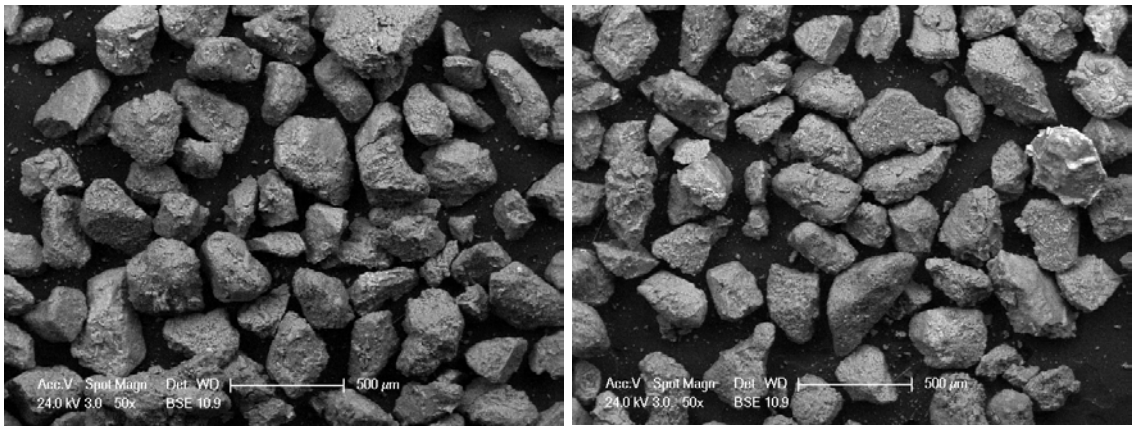

Figure 4.17. SEM image for spent 0.3 mm particle sized 1.5 wt % Pt–5 wt% CeO_2/Al_2O_3 catalyst (50x).

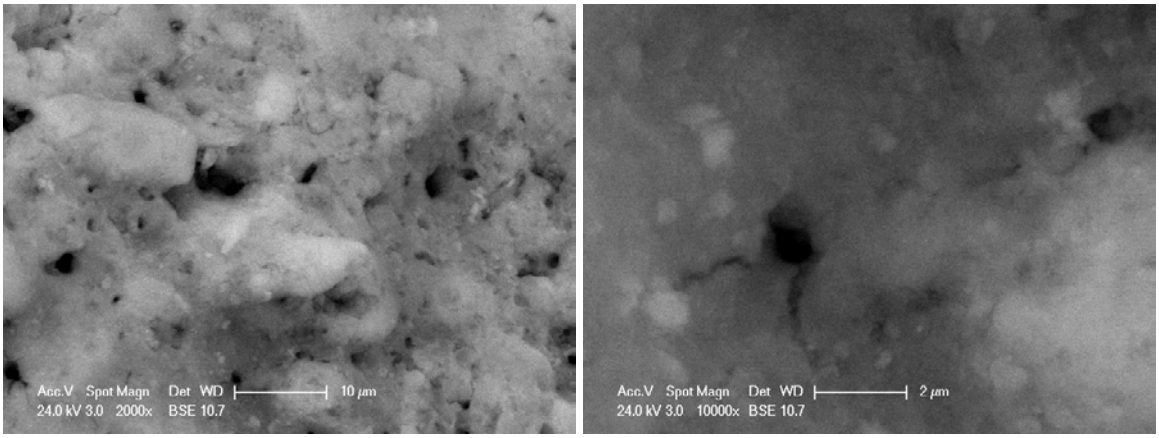

(a) (b)

Figure 4.18. SEM image for spent 0.3 mm particle sized 1.5 wt % Pt–5 wt% CeO_2/Al_2O_3 catalyst a. Magnified 2000x b. Magnified 10000x.

5. CONCLUSIONS AND RECOMMENDATIONS

5.1. Conclusions

In this study, parametric investigation of LT-WGS over Pt-based catalysts is carried out. The effects of reaction temperature, feed conditions, catalyst particle size and reactor geometry on CO conversion are investigated. $Pt/CeO_2/Al_2O_3$ and Pt/MIL-53(Al) are used as catalysts, both of which are prepared by the incipient-to-wetness impregnation method. In each experiment, CO conversion defined as Equation 3.1 is reported. Catalyst surface characterization for $Pt/CeO_2/Al_2O_3$ catalyst is done by using SEM and EDX analyses, whereas XRD analysis is carried out for MIL-53(Al) and Pt/MIL-53(Al) to observe their crystal structures. The conclusions of the study are summarized as follows:

- CO conversion increases with temperature. Highest conversion is found to be 84 % at 325 °C with a feed composition involving highest amount of CO_2.
- It is observed that Pt-based catalysts work inefficiently at 250°C, whereas they start to show catalytic activity at temperatures 300 °C and above.
- It is observed that amount of product gas in the feed composition affects the CO conversion. The feed composition involving presence of equal amounts of product gases provide the lowest conversion theoretically, which is consistent with experimental results. Moreover, highest amount of CO_2 in the feed composition provides the highest conversion. This finding is linked with the positive correlation of CO_2 with ceria activity..
- CO conversion is higher in the absence of H_2 and CO_2 due to the thermodynamic constraints involved in WGS in which the forward reaction is favored.
- It is concluded that the storage conditions of MIL-53 (Al) is crucial to abstain the possible degeneration on its structure.
- The effect of catalyst preparation on structure of MIL-53 (Al) is another significant finding. Incipient-to-wetness impregnation method may be an improper technique for catalyst preparation involving MIL-53 (Al) as the support material.

- It is found out that the presence of ceria makes the catalyst unsuitable for coating it on the FeCrAlY plates for microchannel applications. This is believed to be due to water affinity of ceria, which cause the adsorption of H_2O molecules in the feed.
- In micro packed configuration, channeling between metal housing and quartz reactor is a possible issue, which should be overcomed for further studies.
- The effect of diluting the catalyst bed with Al_2O_3 on CO conversion is another important conclusion. It is observed that the CO conversion increases with amount of diluent in the dilution.
- Reactor diameter is found to affect CO conversion, which changed from 1 % and 4 % upon decreasing the diameter from 10 mm to 2 mm. The improvement in the conversion is believed to be due to the better mixing conditions in the catalyst bed.
- It is observed that the CO conversion decreases from 12 % to 1 % with increasing catalyst particle size, which is changed from $3.02x10^{-1}$ mm to $3x10^{-3}$ mm. Smaller particles provide more surface area and an intraparticle diffusion resistance free environment which increases the interaction between molecules and catalyst.
- In SEM analysis, it is observed that porous structure of the catalyst is unaffected by the reduction and reaction conditions. Moreover, no coke formation is observed on the catalyst surface, which is supported by EDX analysis.
- In EDX analysis, the Ce atoms are at the target value, whereas the Pt atoms are not in the desired value due to the accuracy problems in the analysis machine. Moreover, no agglomeration occurrence is obtained from EDX mapping.

5.2. Recommendations

Regarding the results of present work, following studies are recommended for obtaining further useful results:

- Preparation method of MIL-53(Al) supported catalyst can be improved. The possible alternative methods are chemical vapor deposition and solid grinding, both of which provide improved metal dispersion. Solid grinding can address the degeneracy of MIL-53(Al) after impregnation.
- Ceria can be used as support material for further studies. It promoted to CO conversion significantly, which makes it a promising support for WGS reaction.

- As an alternative active metal, Au can be used in the future study. It is known that Au particles provide high catalytic activity at temperatures 180 ℃ and above, which could address the low conversion at 250 ℃ in this study.
- The effect of feed compositions can be further investigated such as effect of H_2 or CO_2 individually. Moreover, CH_4 can be added to the feed gas to achieve a more realistic feed.

APPENDIX A: MFC CALIBRATION CURVES

MFC calibration curves for all reactant and product gases are introduced in this section.

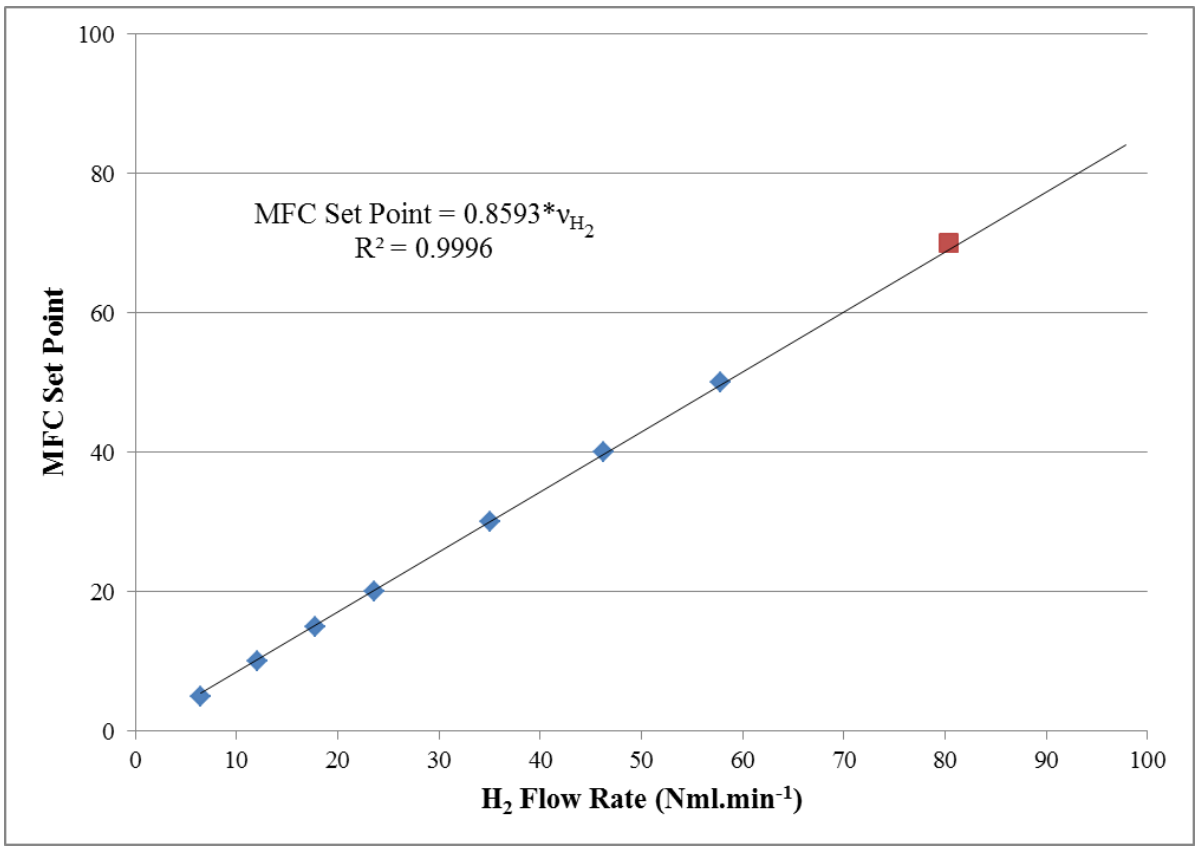

Figure A.1. MFC Calibration Curve of H_2.

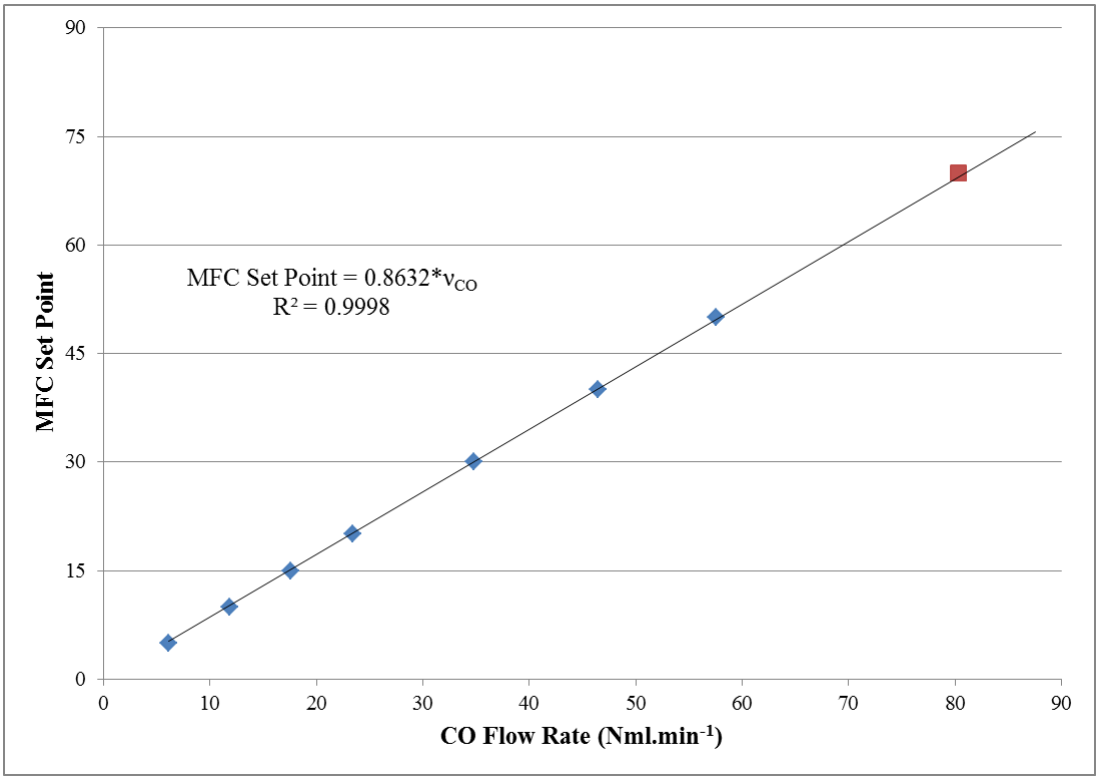

Figure A.2. MFC Calibration Curve of CO.

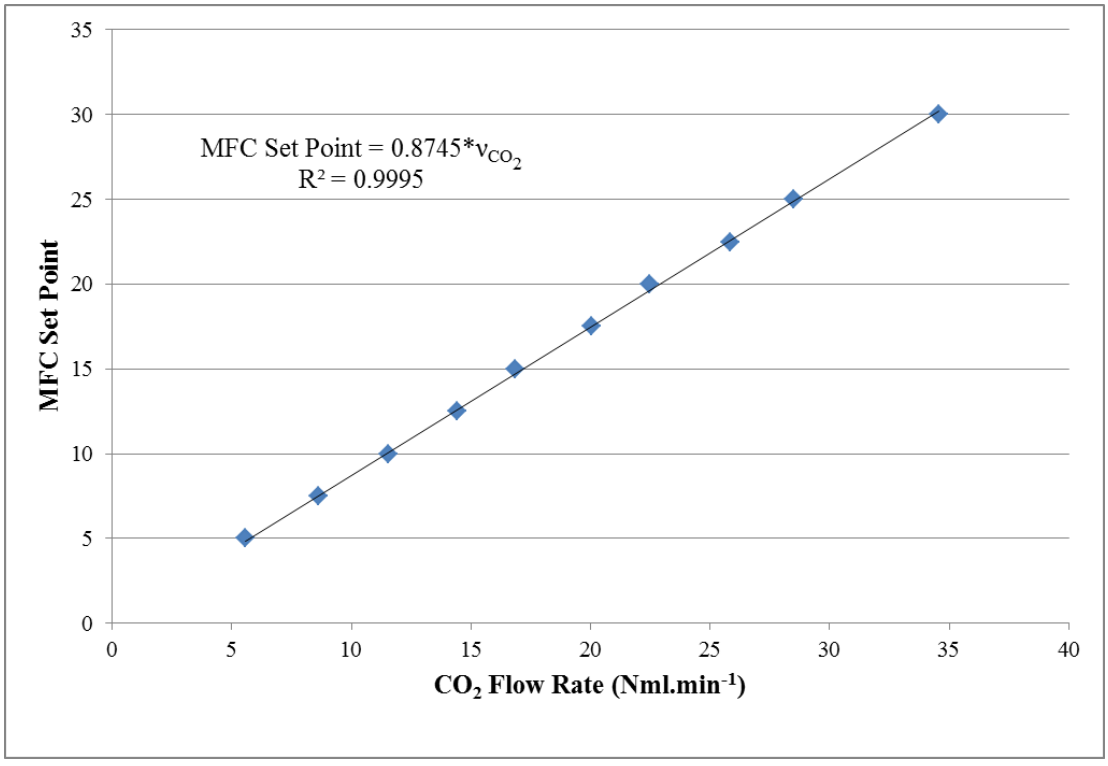

Figure A.3. MFC Calibration Curve of CO_2.

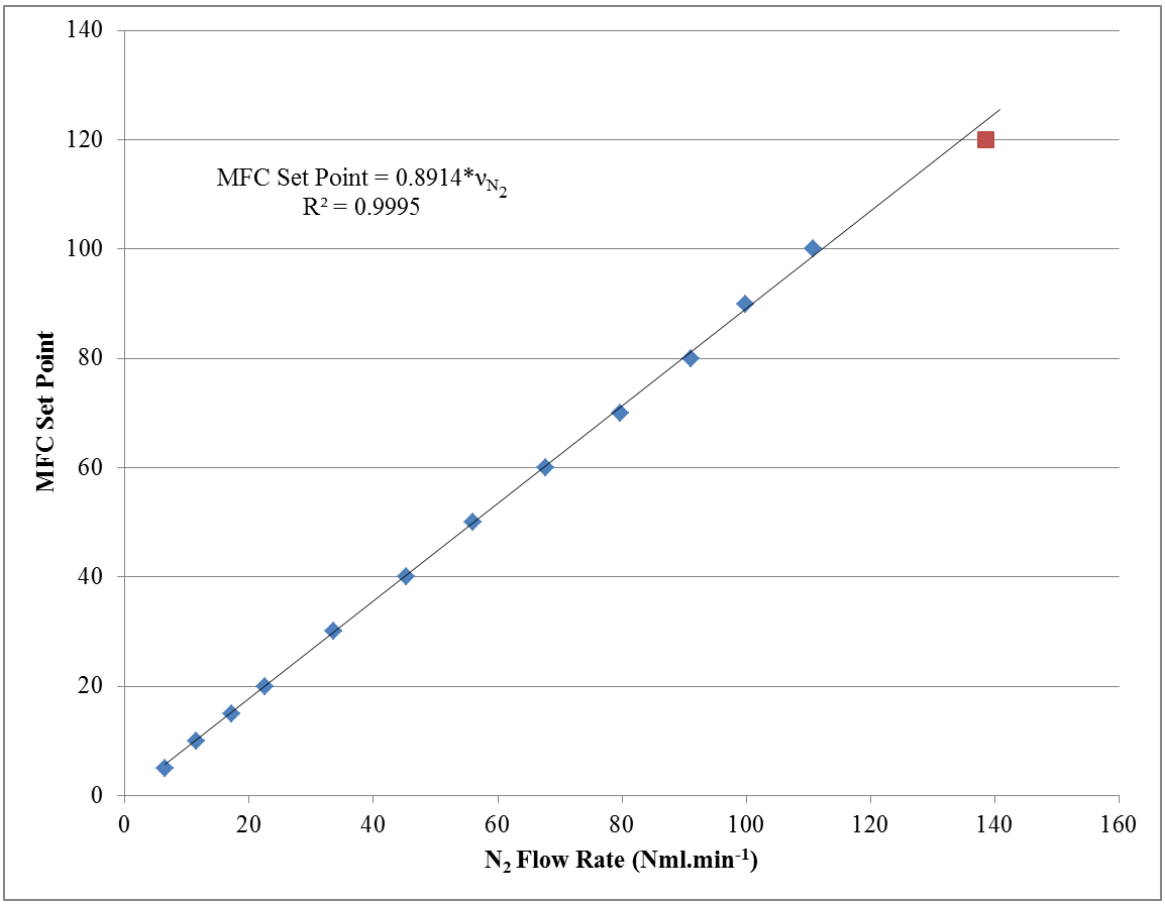

Figure A.4. MFC Calibration Curve of N_2.

APPENDIX B: GC CALIBRATION CURVES

GC calibration curves for all reactant and product gases are introduced in this section.

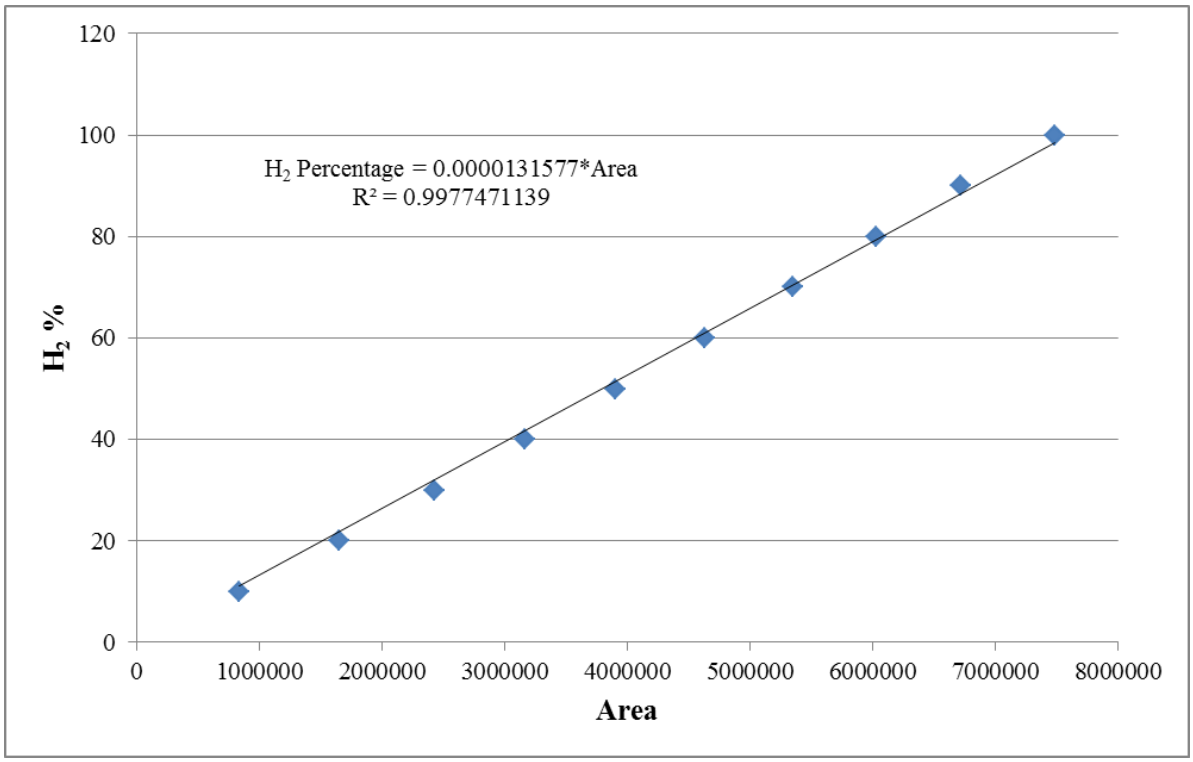

Figure B.1. GC Calibration Curve for H_2.

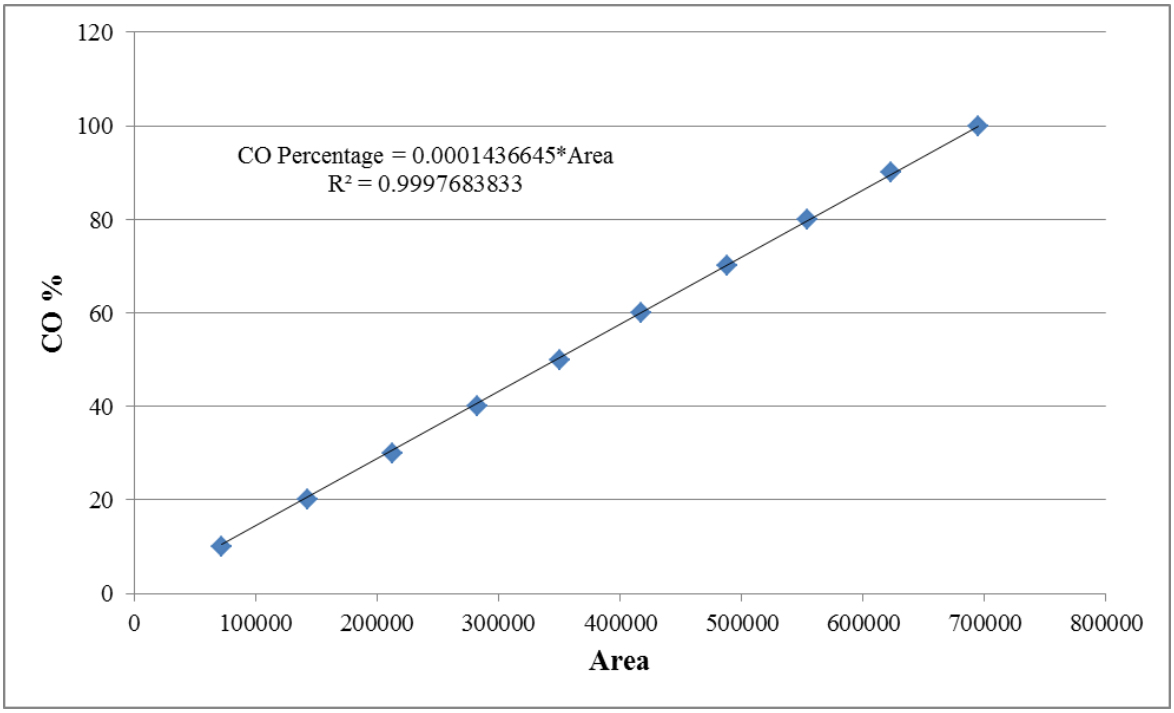

Figure B.2. GC Calibration Curve for CO.

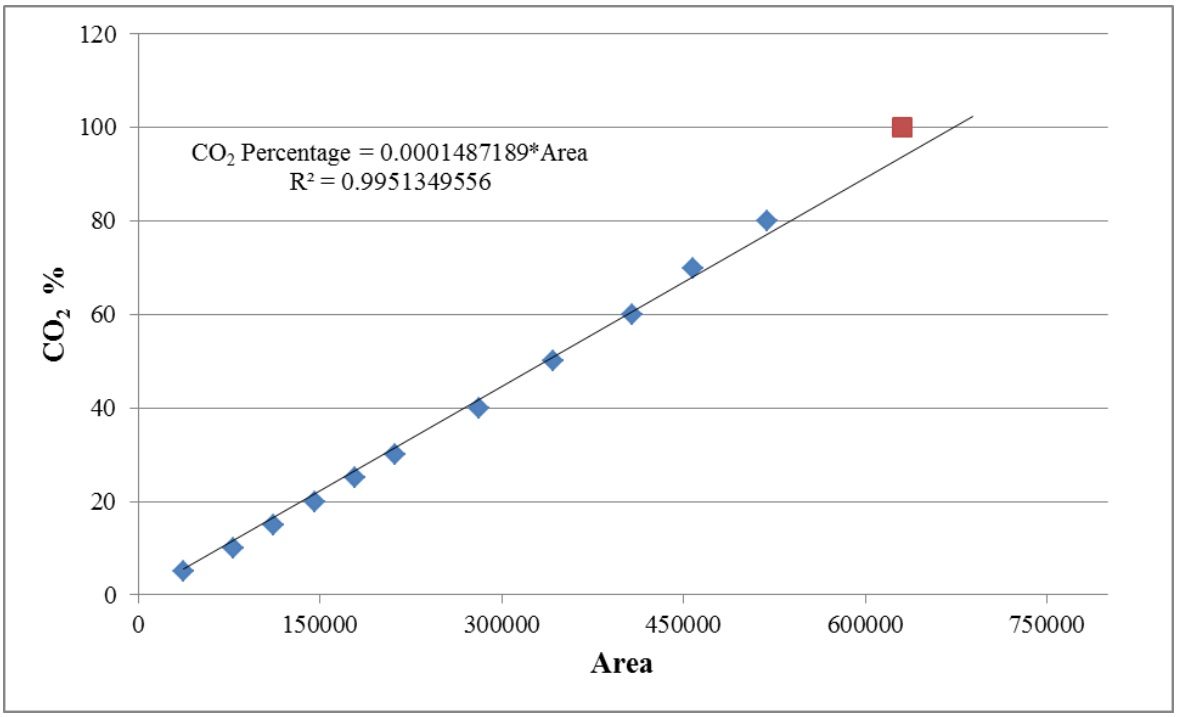

Figure B.3. GC Calibration Curve for CO_2

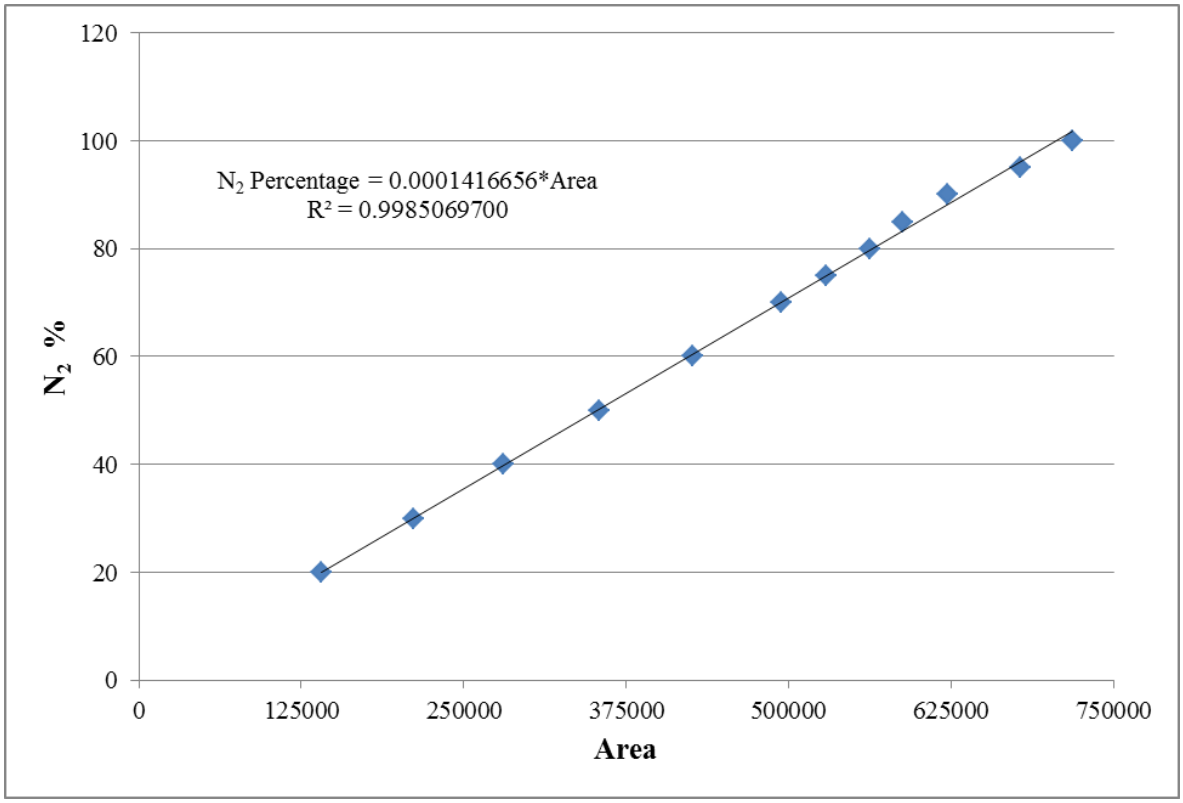

Figure B.4. GC Calibration Curve of N_2.

REFERENCES

Andreeva, D., I. Ivanov, L. Ilieva, J. W. Sobczak, G. Avdeev, and K. Petrov, "Gold Based Catalysts on Ceria and Ceria-Alumina for Wgs Reaction (Wgs Gold Catalysts)", *Topics in Catalysis*, Vol. 44, No. 1-2, pp. 173-182, 2007.

Azzam, K. G., I. V. Babich, K. Seshan, and L. Lefferts, "A Bifunctional Catalyst for the Single-Stage Water-Gas Shift Reaction in Fuel Cell Applications. Part 2. Roles of the Support and Promoter on Catalyst Activity and Stability", *Journal of Catalysis*, Vol. 251, No. 1, pp. 163-171, 2007.

Baier, T. and G. Kolb, "Temperature Control of the Water Gas Shift Reaction in Microstructured Reactors", *Chemical Engineering Science*, Vol. 62, No. 17, pp. 4602-4611, 2007.

Ball, M. and M. Wietschel, "The Future of Hydrogen - Opportunities and Challenges", *International Journal of Hydrogen Energy*, Vol. 34, No. 2, pp. 615-627, 2009.

Boaro, M., M. Vicario, J. Llorca, C. de Leitenburg, G. Dolcetti, and A. Trovarelli, "A Comparative Study of Water Gas Shift Reaction over Gold and Platinum Supported on ZrO_2 and CeO_2-ZrO_2", *Applied Catalysis B-Environmental*, Vol. 88, No. 3-4, pp. 272-282, 2009.

Chen, W. H., T. C. Hsieh, and T. L. Jiang, "An Experimental Study on Carbon Monoxide Conversion and Hydrogen Generation from Water Gas Shift Reaction", *Energy Conversion and Management*, Vol. 49, No. 10, pp. 2801-2808, 2008.

Chen, W. H., M. R. Lin, T. L. Jiang, and M. H. Chen, "Modeling and Simulation of Hydrogen Generation from High-Temperature and Low-Temperature Water Gas Shift Reactions", *International Journal of Hydrogen Energy*, Vol. 33, No. 22, pp. 6644-6656, 2008.

Commenge J. M., L. Falk, J.P. Corriou and M. Matlosz, "Optimal Design for Flow Uniformity in Microchannel Reactors", *AlChE Journal*, Wiley, Vol.44, No.2, 2004.

Cychosz, K. A., A. G. Wong-Foy, and A. J. Matzger, "Liquid Phase Adsorption by Microporous Coordination Polymers: Removal of Organosulfur Compounds", *Journal of the American Chemical Society*, Vol. 130, No. 22, pp. 6938-6939, 2008.

Ehrfeld, W., V. Hessel and H. Löwe, "Microreactors: New Technology for Modern Chemistry", WILEY-VCH Verlag GmbH, Weinheim, Germany, 2001.

Ertem, Ö., "Parametric Investigation of Water Gas Shift Over Pd Based Catalysts", M.S. Thesis, Boğaziçi University, 2014.

Farha, O. K., A. O. Yazaydin, I. Eryazici, C. D. Malliakas, B. G. Hauser, M. G. Kanatzidis, S. T. Nguyen, R. Q. Snurr, and J. T. Hupp, "De Novo Synthesis of a Metal-Organic Framework Material Featuring Ultrahigh Surface Area and Gas Storage Capacities", *Nature Chemistry*, Vol. 2, No. 11, pp. 944-948, 2010.

Farrusseng, D., S. Aguado, and C. Pinel, "Metal-Organic Frameworks: Opportunities for Catalysis", *Angewandte Chemie-International Edition*, Vol. 48, No. 41, pp. 7502-7513, 2009.

Fichtner, M., J. Mayer, D. Wolf, and A. Schubert, "Microstructured Rhodium Catalysts for the Partial Oxidation of Methane to Syngas under Pressure", *Industrial & Engineering Chemistry Research*, Vol. 40, No. 16, pp. 3475-3483, 2001.

Fu, Q., W. L. Deng, H. Saltsburg, and M. Flytzani-Stephanopoulos, "Activity and Stability of Low-Content Gold-Cerium Oxide Catalysts for the Water-Gas Shift Reaction", *Applied Catalysis B-Environmental*, Vol. 56, No. 1-2, pp. 57-68, 2005.

Fu, Q., A. Weber, and M. Flytzani-Stephanopoulos, "Nanostructured Au-CeO_2 Catalysts for Low-Temperature Water-Gas Shift", *Catalysis Letters*, Vol. 77, No. 1-3, pp. 87-95, 2001.

Goerke, O., P. Pfeifer, and K. Schubert, "Water Gas Shift Reaction and Selective Oxidation of CO in Microreactors", *Applied Catalysis a-General*, Vol. 263, No. 1, pp. 11-18, 2004.

Henschel, A., K. Gedrich, R. Kraehnert, and S. Kaskel, "Catalytic Properties of MIL-101", *Chemical Communications*, Vol. 35, pp. 4192-4194, 2008.

Hoskins, B. F. and R. Robson, "Infinite Polymeric Frameworks Consisting of 3 Dimensionally Linked Rod-Like Segments", *Journal of the American Chemical Society*, Vol. 111, No. 15, pp. 5962-5964, 1989.

Hwang, K. R., C. B. Lee, and J. S. Park, "Advanced Nickel Metal Catalyst for Water-Gas Shift Reaction", *Journal of Power Sources*, Vol. 196, No. 3, pp. 1349-1352, 2011.

Ishida, T., M. Nagaoka, T. Akita, and M. Haruta, "Deposition of Gold Clusters on Porous Coordination Polymers by Solid Grinding and Their Catalytic Activity in Aerobic Oxidation of Alcohols", *Chemistry-a European Journal*, Vol. 14, No. 28, pp. 8456-8460, 2008.

Jeong, D. W., W. J. Jang, J. O. Shim, W. B. Han, H. S. Roh, U. H. Jung, and W. L. Yoon, "Low-Temperature Water-Gas Shift Reaction over Supported Cu Catalysts", *Renewable Energy*, Vol. 65, No. pp. 102-107, 2014.

Kalamaras, C. M., I. D. Gonzalez, R. M. Navarro, J. L. G. Fierro, and A. M. Efstathiou, "Effects of Reaction Temperature and Support Composition on the Mechanism of Water-Gas Shift Reaction over Supported-Pt Catalysts", *Journal of Physical Chemistry C*, Vol. 115, No. 23, pp. 11595-11610, 2011.

Kam, R., J. Scott, R. Amal, and C. Selomulya, "Pyrophoricity and Stability of Copper and Platinum Based Water-Gas Shift Catalysts During Oxidative Shut-Down/Start-up Operation", *Chemical Engineering Science*, Vol. 65, No. 24, pp. 6461-6470, 2010.

Karakaya M., "Experimental and Quantitative Analysis of Multiphase Catalytic Reactions under Microfluidic Flow Conditions and Geometries", Ph.D. Thesis, Boğaziçi University, 2012.

Karakaya, M., S. Keskin and A. K. Avcı,"Parametric Study of Methane Steam Reforming to Syngas in a Catalytic Microchannel Reactor", *Applied Catalysis A: General*, Vol. 411-412, pp. 114-122, 2012.

Keiski, R. L. and T. Salmi, "Deactivation of the High-Temperature Water Gas Shift Catalyst in Nonisothermal Conditions", *Applied Catalysis a-General*, Vol. 87, No. 2, pp. 185-203, 1992.

Khan, N. A., Z. Hasan, and S. H. Jhung, "Adsorptive Removal of Hazardous Materials Using Metal-Organic Frameworks (MOFs): A Review", *Journal of Hazardous Materials*, Vol. 244, No. pp. 444-456, 2013.

Kim, S. H., S. W. Nam, T. H. Lim, and H. I. Lee, "Effect of Pretreatment on the Activity of Ni Catalyst for CO Removal Reaction by Water-Gas Shift and Methanation", *Applied Catalysis B-Environmental*, Vol. 81, No. 1-2, pp. 97-104, 2008.

Langmi, H. W., J. W. Ren, B. North, M. Mathe, and D. Bessarabov, "Hydrogen Storage in Metal-Organic Frameworks: A Review", *Electrochimica Acta*, Vol. 128, No. pp. 368-392, 2014.

Lee, D. W., M. S. Lee, J. Y. Lee, S. Kim, H. J. Eom, D. J. Moon, and K. Y. Lee, "The Review of Cr-Free Fe-Based Catalysts for High-Temperature Water-Gas Shift Reactions", *Catalysis Today*, Vol. 210, No. pp. 2-9, 2013.

Lee, J., O. K. Farha, J. Roberts, K. A. Scheidt, S. T. Nguyen, and J. T. Hupp, "Metal-Organic Framework Materials as Catalysts", *Chemical Society Reviews*, Vol. 38, No. 5, pp. 1450-1459, 2009.

Lenite, B. A., C. Galletti, and S. Specchia, "Studies on Au Catalysts for Water Gas Shift Reaction", *International Journal of Hydrogen Energy*, Vol. 36, No. 13, pp. 7750-7758, 2011.

LeValley, T. L., A. R. Richard, and M. H. Fan, "The Progress in Water Gas Shift and Steam Reforming Hydrogen Production Technologies - a Review", *International Journal of Hydrogen Energy*, Vol. 39, No. 30, pp. 16983-17000, 2014.

Low, J. J., A. I. Benin, P. Jakubczak, J. F. Abrahamian, S. A. Faheem, and R. R. Willis, "Virtual High Throughput Screening Confirmed Experimentally: Porous Coordination Polymer Hydration", *Journal of the American Chemical Society*, Vol. 131, No. 43, pp. 15834-15842, 2009.

Luengnaruemitchai, A., S. Osuwan, and E. Gulari, "Comparative Studies of Low-Temperature Water-Gas Shift Reaction over Pt/CeO_2, Au/CeO_2, and Au/Fe_2O_3 Catalysts", *Catalysis Communications*, Vol. 4, No. 5, pp. 215-221, 2003.

Noor, T., M. V. Gil, and D. Chen, "Production of Fuel-Cell Grade Hydrogen by Sorption Enhanced Water Gas Shift Reaction Using Pd/Ni-Co Catalysts", *Applied Catalysis B-Environmental*, Vol. 150, No. pp. 585-595, 2014.

Nuzhdin, A. L., K. A. Kovalenko, D. N. Dybtsev, and G. A. Bukhtiyarova, "Removal of Nitrogen Compounds from Liquid Hydrocarbon Streams by Selective Sorption on Metal-Organic Framework Mil-101", *Mendeleev Communications*, Vol. 20, No. 1, pp. 57-58, 2010.

Opelt, S., S. Turk, E. Dietzsch, A. Henschel, S. Kaskel, and E. Klemm, "Preparation of Palladium Supported on MOF-5 and Its Use as Hydrogenation Catalyst", *Catalysis Communications*, Vol. 9, No. 6, pp. 1286-1290, 2008.

Qian, X. K., B. L. Yadian, R. B. Wu, Y. Long, K. Zhou, B. Zhu, and Y. Z. Huang, "Structure Stability of Metal-Organic Framework MIL-53 (Al) in Aqueous

Solutions", *International Journal of Hydrogen Energy*, Vol. 38, No. 36, pp. 16710-16715, 2013.

Rase H. F., *Chemical Reactor Design for Process Plants: Volume two – Case Studies and Design Data*, John Wiley & Sons, 1977

Ratnasamy, C. and J. P. Wagner, "Water Gas Shift Catalysis", *Catalysis Reviews-Science and Engineering*, Vol. 51, No. 3, pp. 325-440, 2009.

Rhodes, C., G. J. Hutchings, and A. M. Ward, "Water-Gas Shift Reaction - Finding the Mechanistic Boundary", *Catalysis Today*, Vol. 23, No. 1, pp. 43-58, 1995.

Serre, C., F. Millange, C. Thouvenot, M. Nogues, G. Marsolier, D. Louer, and G. Ferey, "Very Large Breathing Effect in the First Nanoporous Chromium(III)-Based Solids: MIL-53 or $C^{III}(OH)\cdot\{O_2C\text{-}C_6H_4\text{-}CO_2\}\cdot\{HO_2C\text{-}C_6H_4\text{-}CO_2H\}_x\cdot H_2O_y$", *Journal of the American Chemical Society*, Vol. 124, No. 45, pp. 13519-13526, 2002.

Shekhawat, D., J. J. Spivey, and D. A. Berry, "Fuel Cells: Technologies for Fuel Processing Preface", *Fuel Cells: Technologies for Fuel Processing*, Vol. pp. Vii-Viii, 2011.

Smith, R. J. B., M. Loganathan, and M. S. Shantha, "A Review of the Water Gas Shift Reaction Kinetics", *International Journal of Chemical Reactor Engineering*, Vol. 8, No. pp. 2010.

Thinon, O., F. Diehl, P. Avenier, and Y. Schuurman, "Screening of Bifunctional Water-Gas Shift Catalysts", *Catalysis Today*, Vol. 137, No. 1, pp. 29-35, 2008.

Trimm, D. L., "Minimisation of Carbon Monoxide in a Hydrogen Stream for Fuel Cell Application", *Applied Catalysis a-General*, Vol. 296, No. 1, pp. 1-11, 2005.

Turner, J. A., "Sustainable Hydrogen Production", *Science*, Vol. 305, No. 5686, pp. 972-974, 2004.

Wang, F., B. Qi, G. Q. Wang, and L. J. Li, "Methane Steam Reforming: Kinetics and Modeling over Coating Catalyst in Micro-Channel Reactor", *International Journal of Hydrogen Energy*, Vol. 38, No. 14, pp. 5693-5704, 2013.

Wang, Q. Y., G. F. Li, B. Zhao, and R. X. Zhou, "The Effect of Rare Earth Modification on Ceria-Zirconia Solid Solution and Its Application in Pd-Only Three-Way Catalyst", *Journal of Molecular Catalysis a-Chemical*, Vol. 339, No. 1-2, pp. 52-60, 2011.

Wang, Q. Y., B. Zhao, G. F. Li, and R. X. Zhou, "Application of Rare Earth Modified Zr-Based Ceria-Zirconia Solid Solution in Three-Way Catalyst for Automotive Emission Control", *Environmental Science & Technology*, Vol. 44, No. 10, pp. 3870-3875, 2010.

Watts, P. and C. Wiles, "Recent Advances in Synthetic Micro Reaction Technology", *Chemical Communications*, Vol. 5, pp. 443-467, 2007.

Wheeler, C., A. Jhalani, E. J. Klein, S. Tummala, and L. D. Schmidt, "The Water-Gas-Shift Reaction at Short Contact Times", *Journal of Catalysis*, Vol. 223, No. 1, pp. 191-199, 2004.

Zalc, J. M. and D. G. Loffler, "Fuel Processing for Pem Fuel Cells: Transport and Kinetic Issues of System Design", *Journal of Power Sources*, Vol. 111, No. 1, pp. 58-64, 2002.